OPTICAL HYPERFINE STRUCTURE STUDIES IN CADMIUM AND IN BARIUM

by

Edward Tomchuk

A Thesis Presented to the
Faculty of Graduate Studies
and Research
University of Manitoba
in Conformity
with the Requirements for the
PhD Degree

October 1964

ABSTRACT

Optical hyperfine structures have been observed in cadmium and barium by means of an atomic beam light source together with a Fabry-Perot interferometer.

The CdI singlet resonance line $\lambda 2288 A^{o}$ ($5s^2\ {}^1S_o$ - $5s5p\ {}^1P_1$) showed three components A, B and C in order of decreasing frequency. The measured separations were

$$\Delta\gamma(A,B) = 16.8 \pm 0.3 \text{ mK}$$

$$\Delta\gamma(B,C) = 12.5 \pm 0.5 \text{ mK}$$

The isotopes 110 and 111 were assigned to component A; 112 and 113, to component B; and 114, to component C. The isotope shifts in this line together with the isotope shifts in the CdI intercombination line $\lambda 3261 A^{o}$ ($5s^2\ {}^1S_o$ - $5s5p\ {}^3P_1$) which had been measured previously were analyzed in the manner of Crawford et al. It was found that the specific mass integral

$$K(5s, 5p) = - 0.03 \pm 0.03$$

On comparing this integral with others of the form K(ns, np) it was observed that these integrals were not very sensitive to the principal quantum number n and for n = 5 the integrals appear to be decreasing in value. Hence, in the heavy elements one can expect to obtain specifically nuclear data from the observed shifts.

The BaI singlet resonance line $\lambda 5535 A^{o}$ ($6s^2\ ^1S_o$ - $6s6p\ ^1P_1$) was resolved into four components A, B, C and D with D having the highest frequency. The measured separations were:

$$\Delta\gamma(A,B) = 4.4 \pm 0.3 \text{ mK}$$

$$\Delta\gamma(A,C) = 10.0 \pm 0.3 \text{ mK}$$

$$\Delta\gamma(A,D) = 18.6 \pm 0.3 \text{ mK}$$

The relative intensities A:B:C:D were 14:4.5:4:1 with an error of 20%. Visual observations indicated the presence of a fifth component between A and B but the resolution was not sufficient to give a numerical value to its position. According to Jackson the structure observed in this line is due to a combination of isotope shift and magnetic hyperfine structure and the order of the isotopes is 138, 136, 134, 137 and 135 with 135 having the highest frequency.

The second member of the principal singlet series in BaI, $\lambda 3072 A^{o}$ was also studied. A wing 15 mK wide was observed on the high frequency of the fringes. The structure of this line is almost entirely due to the magnetic hyperfine structure of the two odd isotopes. The structures of the two BaI lines are consistent.

The BaII resonance lines $\lambda 4934 A^{o}$ and $\lambda 4554 A^{o}$ ($6s\,^{2}S_{1/2}$ - $6p\,^{2}P_{1/2,3/2}$) were studied. The following magnetic hyperfine structure splittings were observed:

	137	135	Ratio
$^{2}S_{1/2}$	269.1 ± 0.6	238.9 ± 1.5	1.126 ± 0.010
$^{2}P_{1/2}$	50.4 ± 0.7	44.8 ± 1.5	1.125 ± 0.056
$^{2}P_{3/2}$(F3-F2)	15.1 ± 0.8	13.3 ± 0.8	1.135 ± 0.128

These ratios agree with the more accurate value 1.119 determined from magnetic resonance experiments. The positions of the isotopes relative to 138 in mK are:

	138	137	136	135	134
$\lambda 4934 A^{o}$	0	+10.1±1.0	+6.7±0.2	+13.0±1.5	+8.7±0.3
$\lambda 4554 A^{o}$ (3cm spacer)	0	+9.8±1.0	+7.2±0.1	+13.1±1.5	+9.6±0.6
(5cm spacer)	0	+9.3±1.0	+7.2±0.1	+12.6±1.5	+9.6±0.6

The results from the 3 cm spacer of $\lambda 4554 A^{o}$ are considered more reliable than the results from the 5 cm spacer, and the results of $\lambda 4934 A^{o}$ more reliable than those of $\lambda 4554 A^{o}$. Although the data is not conclusive on the relative positions of the isotopes, it can be stated that, within the experimental error, the order of the isotopes in both BaII lines is the same as in the BaI line $\lambda 5535 A^{o}$, i.e. 138, 136, 134, 137 and 135.

The isotope shifts in BaII $\lambda 4934 A^{o}$ are compared to the shifts in BaI $\lambda 5535 A^{o}$ determined by Jackson and Duong and are discussed in terms of nuclear theory.

The isotope shift constant was estimated for the ground term of the single valence electron spectrum, BaII $6s\,^{2}S_{1/2}$, for the isotope pair 135, 137 as

$$\beta C_{exp} \text{ (Ba 135, 137)} = 15 \pm 7 \text{ mK}.$$

TABLE OF CONTENTS

Contents continued,

LIST OF FIGURES

LIST OF PLATES

LIST OF TABLES

CHAPTER I

INTRODUCTORY THEORY

1.1 Introduction

Under high resolution many atomic spectral lines are found to consist of a number of closely spaced components. These spectral lines are said to exhibit hyperfine structure. Hyperfine structure can arise from magnetic hyperfine structure or from isotope shift or from a combination of both of these.

Magnetic hyperfine structure is caused by the interaction of the nuclear magnetic moment with the valence electrons resulting in a splitting of the energy levels into a number of hyperfine structure states.

Isotope shift is caused by differential shifts in terms due to differences in the nuclear properties of the isotopes of the same element and can be subdivided into the mass effect and the field or volume effect. Isotope shift in the lighter elements is completely accounted for by the mass effect while isotope shift in the heavier elements arises from the field or volume effect.

The mass effect can be subdivided into the normal mass effect and the specific mass effect. The normal mass effect explains completely the isotope shift in one-electron hydrogenic spectra. In elementary theory it is assumed that the nucleus remains at rest and that the electron moves around a center of mass coincident with the center of force. In fact the nucleus has a finite though large mass and the nucleus and the electron rotate about their common center of mass. The normal mass effect accounts for this by replacing the electronic mass with its reduced mass in the hydrogenic term values. The specific mass effect occurs in atoms with two or more electrons and arises from the interaction between the electrons. It may operate in the same or in the opposite sense to the normal mass effect depending upon whether the electrons ''move'' predominantly in the same or in the opposite direction resulting in an increase or decrease in the nuclear motion which is required to keep the center of mass of the whole atomic system at rest. While the calculation of the normal mass effect is easily performed, the calculation of the specific mass effect involves the evaluation of integrals which are of the same form as those which arise in intensity calculations. The parts of the wave functions used are the tails where they overlap. The difficulties arise because the tails of the wave functions are not always known accurately. Both the normal mass

effect and the specific mass effect decrease with increasing mass number and they become negligibly small for the heaviest elements.

The field or volume effect arises because the nucleus has a finite volume within which the potential ''experienced'' by the electrons departs from that given by the Coulomb law. The departure from the Coulombic potential is least for the isotope of an element with the smallest nuclear radius. Isotope shift in the heavier elements is completely accounted for by the field or volume effect.

Two atomic systems may be defined as having equal energies when the electrons of the systems are at rest at infinity. The isotope shift in a level is then the difference in energy in bringing the electrons together from infinity. In this case, all electrons, including those in closed shells, contribute to the isotope shift of a level.

It is often more useful to define ''equal energy of two isotopes'' as the state in which only one of the outer electrons is removed to infinity. The isotope shift in a level is again the difference in energy in brining the electrons together but in this case only the single electron contributes to the isotope shift of a level.

It should be noted that the observed isotope shifts in spectral lines must be reduced to isotope shifts in levels. To obtain the isotope shift in a level the isotope shift in several spectral lines of a series must be measured and extrapolated to the series limit. This procedure can be omitted if the isotope shift of one of the levels of the transition is negligibly small so that the removal of the outer electron from this level requires the same energy for both isotopes.

The isotope shift observed in a spectral line can be regarded as the difference in the displacements of the lines of the isotopes from the fictitious position they would have if the cause of the effect vanished. The displacement of a line of any one isotope from this fictitious position arises from the difference in the displacements of the two levels of the transition from their fictitious positions. This is shown in Figure 1 and Figure 2.

1.2 Isotope Shift

(i) The mass effect

The mass effect is due to the differences in mass of the isotopes of the same element and can be subdivided into the normal mass effect and the specific mass effect.

The normal mass effect explains completely the isotope shift in one-electron hydrogenic spectra. The finite mass of the nucleus can be accounted for by replacing the mass of the electron with its reduced mass in the hydrogenic term value.

The hydrogenic term value for a nucleus of infinite mass is given by

$$T_\infty = \frac{R_\infty Z^2}{n^2} \qquad (1.1)$$

where T_∞ is the term value for a nucleus of infinite mass

R_∞ is Rydberg's constant for a nucleus of infinite mass

Z is the atomic number

n is the principal quantum number

If the electronic mass m in R_∞ is now replaced by the reduced mass of the electron, μ, where

$$\mu = \frac{mM}{M + m} \qquad (1.2)$$

and M is the mass of the nucleus, the following expressions are obtained for the term value T of a nucleus with a finite mass,

$$T = T_\infty \left(\frac{M}{m + M}\right) = \frac{\mu}{m} T_\infty \qquad (1.3)$$

$$T \approx T_\infty \left(1 - \frac{m}{M}\right) \qquad (1.4)$$

It is obvious from this expression that the term value of the heaviest isotope lies ''lowest'' in the energy level diagram, i.e., has the largest negative energy.

Consider two isotopes with nuclear masses M_1 and M_2 where $M_2 > M_1$. The isotope shift in a term $\delta\Delta T$ is given by

$$\delta\Delta T = m \left(\frac{1}{M_1} - \frac{1}{M_2}\right) T_\infty \approx \frac{m}{m_p} \left(\frac{1}{A_1} - \frac{1}{A_2}\right) T_\infty \qquad (1.5)$$

where mass defects have been neglected, the mass of the proton and neutron has been taken as the same, and hence

$$M \approx A m_p \qquad (1.6)$$

where A is the mass number of an isotope and m_p is the mass of the proton.

The isotope shift in a spectral line due to the normal mass effect is given by

$$\delta\Delta\gamma \approx \frac{m}{m_p} \frac{A_2 - A_1}{A_1 A_2} \gamma \qquad (1.7)$$

where γ is the wave number of the spectral line. The normal mass effect decreases with increasing mass number and is roughly proportional to $\frac{1}{A^2}$. Since the displacement due to the mass effect reduces the term value and since this displacement decreases with increasing A, the spectral line component due to the heavier isotope has the greater wave number. This is shown in Figure 1.

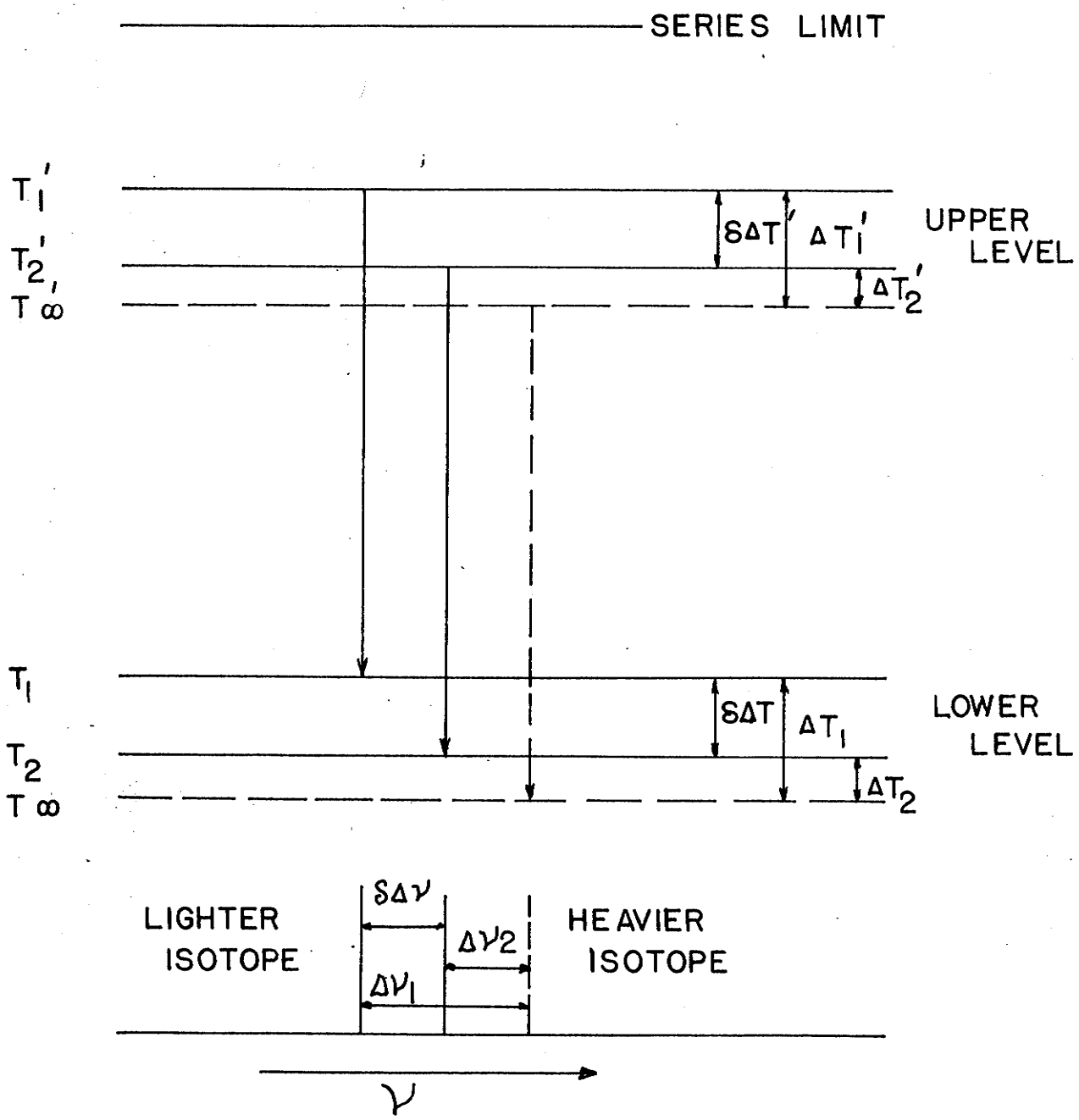

δΔν - ISOTOPE SHIFT (NORMAL MASS EFFECT) IN SPECTRAL LINE
Δν's - DISPLACEMENTS IN SPECTRAL LINE
ΔT's - DISPLACEMENTS IN LEVELS
δΔT - ISOTOPE SHIFT (NORMAL MASS EFFECT) IN TERMS
- - - DASHED LINES SHOW THE FICTITIOUS TERM VALUES AND ASSOCIATE SPECTRAL LINE IF THE NUCLEUS HAD INFINITE MASS

NORMAL MASS EFFECT

FIGURE – 1

The specific mass effect occurs in atoms of several electrons. It arises from the interaction or ''coupling'' of the electrons. It can operate in the same or in the opposite sense to the normal mass effect depending upon whether the electrons ''move'' in predominantly in the same or in the opposite direction resulting in an increased or decreased nuclear motion which is required to keep the center of mass of the whole atomic system at rest.

Consider the atom to consist of a number of electrons, N, each of mass m, and a nucleus of mass M. The kinetic energy of the system is

$$T = \frac{1}{2} m \sum_{k=1}^{N} \dot{\underline{r}}_k^2 + \frac{1}{2} M \dot{\underline{r}}^2 \qquad (1.8)$$

where $\underline{r}_i$ and $\underline{r}$ are the position vectors of the electrons and nucleus relative to a fixed origin. Introduce the position vector $\underline{R}$ of the center mass. Then

$$(M + Nm)\ \underline{R} = M\underline{r} + m \sum_{k=1}^{N} \underline{r}_k \qquad (1.9)$$

Let $\underline{s}_k$ give the position of k^{th} electron relative to the nucleus. Then

$$\underline{s}_k = \underline{r}_k - \underline{r} \qquad (1.10)$$

The kinetic energy of the system when expressed in terms of the momenta $\underline{p}_k$ conjugate to $\underline{s}_k$, and the momentum $\underline{P}$ conjugate to $\underline{R}$ is then

$$T = \frac{1}{2\mu} \sum_{k=1}^{N} p_k^2 + \frac{1}{M} \sum_{k<j} p_k \cdot p_j + \frac{1}{2(M + Nm)} P^2 \qquad (1.11)$$

The kinetic energy operator for a system of N electrons and one nucleus is then

$$T = -\hbar^2 \left\{ \frac{1}{2\mu} \sum_{k=1}^{N} \nabla_k^2 + \frac{1}{M} \sum_{k<j} \nabla_k \cdot \nabla_j + \frac{1}{2(M + N_m)} \nabla^2 \right\} \qquad (1.12)$$

where μ is the reduced mass of the electron

$\nabla_k \equiv \underline{i} \frac{\partial}{\partial x_k} + \underline{j} \frac{\partial}{\partial y_k} + \underline{k} \frac{\partial}{\partial z_k}$ where x_k, y_k, z_k are the coordinates of the k^{th} electron with respect to an origin at the nucleus and

$\nabla \equiv \underline{i}' \frac{\partial}{\partial X} + \underline{j}' \frac{\partial}{\partial Y} + \underline{k}' \frac{\partial}{\partial Z}$ where X, Y, Z are the coordinates of the center of mass in another system of arbitrary fixed origin.

The Schrödinger equation is then

$$\{T + V - W\} \Psi = 0 \qquad (1.13)$$

where V is the potential energy of the atom and is independent of the coordinates of the center of mass.

For simplicity assume that the center of mass is at rest so that Ψ is independent of the center of mass coordinates X, Y, Z. This simplification is justified, i.e., setting $\underline{P}$ equal to zero since in a radiative process the momentum of the photon is very small so that $\underline{P}$ does not change appreciably. The atomic

system has zero energy when all the particles are at rest at infinity. Hence

$$\left\{\frac{\hbar^2}{2\mu}\sum_{k=1}^{N}\nabla_k^2+\frac{\hbar^2}{M}\sum_{k<j}\nabla_k\cdot\nabla_j+W-V\right\}\Psi=0 \qquad (1.14)$$

Assume that the wave functions of the system and the characteristic energy values are known for a nucleus of infinite mass. The small change in energy resulting from the motion of the nucleus of finite mass M can then be treated as a perturbation of the system and can be approximately resolved into two parts corresponding to the normal mass effect which was discussed previously and the specific mass effect. In the above equation the second term represents the mutual coupling of the electrons. It obviously vanishes for the one electron problem. Without this second term the expression is

$$\left\{\frac{\hbar^2}{2\mu}\sum_{k=1}^{N}\nabla_k^2+W-V\right\}\Psi=0 \qquad (1.15)$$

This is simply the extension to the usual hydrogen problem. The electrostatic potential energy is in general

$$V=-\sum_{k=1}^{N}\frac{Ze^2}{r_k}+\sum_{k<j}\frac{e^2}{r_{jk}} \qquad (1.16)$$

The eigenvalues can be found without knowing the wave functions by introducing new variables $x_k'=\frac{\mu}{m}x_k$ etc.

Hence $$W(M) = \frac{\mu}{m} W_\infty \qquad (1.17)$$

where $W(M)$ is the energy level of the atomic system for a nucleus of mass M

W_∞ is the corresponding energy level of the atomic system for a nucleus of infinite mass.

It is easy to show that the above expression can be written as

$$W(M) = W_\infty + \Delta_N W(M) \qquad (1.18)$$

where $\Delta_N W(M)$ is the displacement in the energy due to the normal mass effect

$$\Delta_N W(M) = - \frac{m}{m+M} W_\infty \approx - \frac{m}{M} W_\infty \qquad (1.19)$$

Hence $$W(M) \approx W_\infty (1 - \frac{m}{M}) \qquad (1.20)$$

This is the same result as was obtained previously for the normal mass effect except here the discussion involves energies, W's, whereas, the previous discussion involved term values, T's.

The ''coupling'' term (the specific mass effect) can now be included as a perturbation. The energy level is displaced an additional amount $\Delta_s W(M)$ due to this specific mass effect. Hence

$$W(M) = W_\infty + \Delta_N W(M) + \Delta_s W(M) \qquad (1.21)$$

From first order perturbation theory

$$\Delta_s W(M) = -\frac{\hbar^2}{M}\int \Psi^* \left(\sum_{k<j} \nabla_k \cdot \nabla_j\right) \Psi \, d\tau \qquad (1.22)$$

The specific mass effect can be evaluated only when some assumption is made regarding the wave functions.

Hughes and Eckart[20] have evaluated the specific shift for some simple atoms. They made the simplest assumption possible. They assumed that Ψ is a linear combination of products of single electron wave functions, each with a different nuclear charge determined by the variational method. Two and three electron systems were considered. Isotope shifts have been measured in the lighter elements and it has been found that the Hughes-Eckart theory is at best only a qualitative description of the observed shifts. Excellent agreement is obtained in some cases with a more refined theory which uses variational wave functions[1,6,15,35,45].

Bartlett and Gibbons[5] assumed Russell-Saunders coupling and extended the calculation of the specific mass effect to atoms with any number of electrons. Recall

$$\Delta_s W(M) = -\frac{\hbar^2}{M}\int \Psi^* \left(\sum_{k<j} \nabla_k \cdot \nabla_j\right) \Psi \, d\tau \qquad (1.23)$$

In this treatment Slater's[44] approximation is used. In Slater's approximation the wave function corresponding

to a given level is a determinant function of single electron orthogonal wave functions of the configuration from which the level arises. Hence

$$\Delta_s W(M) = + \frac{2mR_\infty}{M} \sum_{\substack{\text{all pairs} \\ n,n'}} K(n,n') \text{ cm}^{-1} \qquad (1.24)$$

where $K(n,n')$ is in atomic units and is given by

$$K(n,n') = \int u^*(\tfrac{n}{x_k}) u^*(\tfrac{n'}{x_j}) \nabla_j \cdot \nabla_k \, u(\tfrac{n}{x_j}) \, u(\tfrac{n'}{x_k}) \, d\tau_j \, d\tau_k \qquad (1.25)$$

and n and n' represent the sets of single-electron quantum numbers (n, ℓ, m_ℓ, m_s) and $(n', \ell', m'_\ell, m'_s)$ respectively, and $u(\frac{n}{x_k})$ represents a single-electron central field function.

K is intrinsically negative so that $\Delta_s W(M)$ is also intrinsically negative. The specific mass effect $\Delta_s W(M)$ is inversely proportional to the nuclear mass. Hence the energy level of the lightest isotope lies ''lowest'' in an energy level diagram. Whether the frequency of the line emitted by the lighter isotope is higher or lower than that of the heavier isotope depends on the K's of the states involved in the transition.

$$\text{For } K \neq 0, \quad \ell' = \ell \pm 1$$
$$m'_\ell = m_\ell \quad \text{or} \quad m'_\ell = m_\ell \pm 1$$
$$m'_s = m_s \qquad (1.26)$$

that is, the interaction of a pair of electrons in a configuration contributes to the specific mass effect only if

$$\begin{aligned} \Delta\ell &= \pm 1 \\ \Delta m_\ell &= 0, \pm 1 \\ \Delta m_s &= 0 \end{aligned} \qquad (1.27)$$

Bartlett and Gibbons[5] show that the formulae for $K(n,n')$ can be reduced to

$$K(n,\ell,m_\ell;n',\ell-1,m_\ell \pm 1) = \tfrac{1}{2}(\ell \mp m_\ell)(\ell \mp m_\ell - 1)C(n,\ell;n',\ell-1) \qquad (1.28)$$

$$K(n,\ell,m_\ell;n',\ell-1,m_\ell) = (\ell^2 - m_\ell{}^2)C(n,\ell;n',\ell-1) \qquad (1.29)$$

where $C(n,\ell;\ n',\ \ell-1) =$

$$-\left\{\frac{(\ell-1)\int \frac{1}{r} R_{n,\ell}\ R_{n',\ell-1} r^2 dr - \int R_{n',\ell-1} \frac{d}{dr}(R_{n,\ell})\ r^2 dr}{(2\ell-1)(2\ell+1)}\right\}^2 \qquad (1.30)$$

with $R_{n,\ell}$ being the normalized radial part of the single-electron wave function. The partial sum $\sum K$ covering the interaction of a single electron $(n',\ \ell',\ m_\ell')$ with a closed shell (n,ℓ) is, in general, independent of the magnetic quantum number m_ℓ' associated with the single electron. The notation $K(n,\ell\ ;\ n',\ \ell')$ is used to denote this sum. It is a multiple of $C(n,\ell\ ;\ n',\ell')$.

These formulae can now be used to find the isotope shift between the lines of two isotopes of nuclear masses M_1 and M_2 where $M_2 > M_1$. The convention of quoting the shift in wave numbers relative to the lighter isotope will be adopted here.

Consider two energy levels a and b where b has the higher energy.

For M_1 $$W_a(M_1) = W_a + \Delta_N W_a(M_1) + \Delta_s W_a(M_1) \quad (1.31)$$

$$W_b(M_1) = W_b + \Delta_N W_b(M_1) + \Delta_s W_b(M_1) \quad (1.32)$$

The wave number of the line emitted in the transition b -> a is

$$\gamma(M_1) = W_b(M_1) - W_a(M_1) \quad (1.33)$$

$$= W_b - W_a + \Delta_N W_b(M_1) - \Delta_N W_a(M_1) + \Delta_s W_b(M_1) - \Delta_s W_a(M_1) \quad (1.34)$$

$$\therefore \gamma(M_1) = \gamma - \frac{m}{M_1}\gamma + \frac{2mR_\infty}{M_1}\left\{\sum_b K(n,n') - \sum_a K(n,n')\right\} \quad (1.35)$$

where γ is the wave number of the transition for a nucleus of infinite mass.

Similarly for M_2 we have

$$\gamma(M_2) = \gamma - \frac{m}{M_2}\gamma + \frac{2mR_\infty}{M_2}\left\{\sum_b K(n,n') - \sum_a K(n,n')\right\} \quad (1.36)$$

The isotope shift in the line is then

$$\delta\Delta\gamma = \gamma(M_2) - \gamma(M_1) = \delta_N \Delta\gamma + \delta_s\Delta\gamma \qquad (1.37)$$

where the shift due to the normal mass effect

$$\delta_N\Delta\gamma = \gamma m\left(\frac{1}{M_1} - \frac{1}{M_2}\right) \qquad (1.38)$$

and the shift due to the specific mass effect

$$\delta_s\Delta\gamma = 2m\, R_\infty\left\{\sum_a K(n,n') - \sum_b K(n,n')\right\}\left(\frac{1}{M_1} - \frac{1}{M_2}\right) \qquad (1.39)$$

$\delta_N\Delta\gamma$ is always positive but $\delta_s\Delta\gamma$ can be positive or negative depending upon the magnitude of the $K(n,n')$.

It is possible by experiment to estimate the specific mass integrals $K(ns, np)$ by comparing the isotope shifts in the singlet and intercombination resonance lines of certain elements[16,30].

From the specific mass theory[5,16] it is possible to show that the difference in the specific mass shifts is

$$\delta_s\left(\begin{array}{l}\text{intercombination-}\\ \text{singlet resonance}\\ \text{lines}\end{array}\right) = -4mR_\infty\left\{\frac{1}{M_1} - \frac{1}{M_2}\right\} K(ns, np) \qquad (1.40)$$

This expression will be verified for cadmium following Gray's treatment for zinc[16].

For cadmium we have the singlet resonance line $\lambda 2288\text{A}^\circ$ $(5s^2\ {}^1S_o - 5s5p\ {}^1P_1)$ and the intercombination resonance line $\lambda 3261\text{A}^\circ$ $(5s^2\ {}^1S_o - 5s5p\ {}^3P_1)$. The two lines have a common lower level. The upper levels arise from the same 5s5p configuration. The field effect shift of either a $p_{1/2}$ or a $p_{3/2}$ electron is small compared to the shift

due to an s electron so that the shift arising from the field effect should be the same in both of these lines. The specific mass effect predicts that the shifts of these two lines should differ by an amount depending on K(5s, 5p). We have

$$1s^2 2s^2 2p^6 3s^2 3p^6 3d^{10} 4s^2 4p^6 4d^{10} 5s^2\ {}^1S_o \quad (a)$$

$$1s^2 2s^2 2p^6 3s^2 3p^6 3d^{10} 4s^2 4p^6 4d^{10} 5s5p\ {}^1P_1 \quad (b')$$

$$1s^2 2s^2 2p^6 3s^2 3p^6 3d^{10} 4s^2 4p^6 4d^{10} 5s5p\ {}^3P_1 \quad (b'')$$

Then

$$\begin{aligned}\sum_a K(n,n') = {} & 6K(1s,2p)+6K(1s,3p)+6K(1s,4p)+6K(2a,2p) \\ & +6K(2s,3p)+6K(2s,4p)+2K(2p,3s)+10K(2p,3d) \\ & +2K(2p,4s)+10K(2p,4d)+2K(2p,5s)+6K(3s,3p) \\ & +6K(3s,4p)+10K(3p,3d)+2K(3p,4s)+10K(3p,4d) \\ & +2K(3p,5s)+6K(3d,4p)+6K(4s,4p)+10K(4p,4d) \\ & +2K(4p,5s) \\ = {} & X + 2K(2p,5s)+2K(3p,5s)+2K(4p,5s)\end{aligned} \qquad (1.41)$$

where X denotes the sum of all integrals not involving the valence electrons. Note for example K(3d,4p) represents the contribution of a 4p electron interacting with the complete 3d shell and since there are six 4p electrons the integral is multiplied by six.

$\sum_{b'}$ K(n,n') and $\sum_{b'}$, K(n,n') may not be written down in such a straightforward manner as $\sum_{a}$ K(n,n') since the contribution of the 5s,5p pair of electrons is not the same in both levels. We write down the wave functions of the strong field states of the 5s5p configuration using Slater's notation.

		Σm_ℓ	Σm_s
1.	(511; 500)( )	1	1
2.	(510; 500)( )	0	1
3.	(51-1;500)( )	-1	1
4.	( )(511; 500)	1	-1
5.	( )(510; 500)	0	-1
6.	( )(51-1;500)	-1	-1
7.	(511)(500)	1	0
8.	(510)(500)	0	0
9.	(51-1)(500)	-1	0
10.	(500)(511)	1	0
11.	(500)(510)	0	0
12.	(500)(51-1)	-1	0

In Slater's notation the quantum numbers n, ℓ , m_ℓ , of the individual electrons are written in the left hand bracket if $m_s = +\frac{1}{2}$ and in the right hand bracket if $m_s = -\frac{1}{2}$. Since K(n,n') has a value only if $m_s = m_s'$, only pairs of electrons appearing in the same bracket can contribute to the sum.

The first six wave functions can belong only to the triplet level. Any one of them can be used to calculate $\sum_{b'}$, $K(n,n')$. Hence

$$\begin{aligned}\sum_{b'}, K(n,n') = X + [&K(2p,5s) + K(3p,5s) + K(4p,5s) \\ &+ K(1s,5p) + K(2s,5p) + K(3s,5p) \\ &+ K(4s,5p) + K(3d,5p) + K(4d,5p)] \\ &+ K(5s,5p) \\ &= X + Y + K(5s,5p) \qquad (1.42)\end{aligned}$$

where Y is the sum in the square brackets.

The last six wave functions belong to both the triplet and singlet levels. The sum $\sum_{b'} K(n,n') + \sum_{b'}, K(n,n')$ is equal to the sum of the interactions calculated for any two functions with the same values of Σm_ℓ and Σm_s so

$$\sum_{b'} K(n,n') + \sum_{b'}, K(n,n') = 2(X + Y) \qquad (1.43)$$

$$\therefore \quad \sum_{b'}, K(n,n') = X + Y - K(5s,5p) \qquad (1.44)$$

Note that the single electron wave functions of the core electrons are in general slightly different in the $5s^2$ and 5s5p configurations. For example K(2p,3s) has different values for the two configurations. However, Bartlett and Gibbons[5] have shown by calculation for neon that the differences introduced are negligible. It is assumed that this is true here.

The specific mass shift for the singlet transition is

$$\delta_s \Delta\gamma' = 2R_\infty m \left\{ \sum_a K(n,n') - \sum_{b'} K(n,n') \right\} \left(\frac{1}{M_1} - \frac{1}{M_2}\right)$$

$$= -2 R_\infty m \left\{ Y - K(5s,5p) - 2K(2p,5s) - 2K(3p,5s) - 2K(4p,5s) \right\} \left(\frac{1}{M_1} - \frac{1}{M_2}\right) \quad (1.45)$$

The specific mass shift for the intercombination transition is

$$\delta_s \Delta\gamma'' = 2R_\infty m \left\{ \sum_a K(n,n') - \sum_{b''} K(n,n') \right\} \left(\frac{1}{M_1} - \frac{1}{M_2}\right)$$

$$= 2R_\infty m \left\{ Y + K(5s,5p) - 2K(2p,5s) - 2K(3p,5s) - 2K(4p,5s) \right\} \left(\frac{1}{M_1} - \frac{1}{M_2}\right) \quad (1.46)$$

Hence the isotope shift difference due to the specific mass effect is δ(intercombination-singlet resonance lines) =

$$\delta_s \Delta\gamma'' - \delta_s \Delta\gamma' = -4mR_\infty \left(\frac{1}{M_1} - \frac{1}{M_2}\right) K(5s,5p) \quad (1.47)$$

As the integral K(5s,5p) is intrinsically negative

$$\delta_s \Delta\gamma'' > \delta_s \Delta\gamma'$$

This means that because of the specific mass effect the wave number shift of the component due to the heavier isotope relative to that due to the lighter isotope, is algebraically greater in the intercombination line than in the singlet line.

The term shift due to both mass effects is proportional to $\frac{1}{M}$. The normal mass effect decreases with increasing mass number. Its calculation is, however, easily performed and it can be accounted for in any observation. The specific mass effect can be expected to decrease with increasing mass number but it could increase with increasing mass number because of the increasing number of specific mass integrals involved. The present work and one of the associated papers[30] show that the decrease in the specific mass effect in a term due to $\frac{1}{M}$ wins out for K(ns,np) integrals. This is good evidence that above the middle of the periodic table for elements it is safe to assume that the specific mass effect is of the order of magnitude of the normal mass effect and that both mass effects become negligible for the heavy elements.

While the calculation of the normal mass effect is easily performed, the calculation of the specific mass effect is difficult as it involves the computation of integrals involving products of radial wave functions. In a few cases, for example helium, the agreement between theory and experiment has been good. In most cases it is poor. Thus in MgI the calculated shifts are only one half the experimental shifts[49,50]. The reasons for the poor theoretical values may be poor wave functions and the approximate character of the theory.

(ii) The field or volume effect

The field or volume effect arises because the nucleus is not a point charge but has a finite volume within which the potential ''experienced'' by the electrons departs from the Coulomb potential. The isotope shift in the heavier elements is accounted for by the field or volume effect.

According to Kuhn[35] any complete nuclear theory must explain the following characteristics of the field or volume effect:

1) It is essentially the electron configuration of the two levels of a transition which determines the magnitude of the field or volume shift. Appreciable shifts are observed only when the number of s-electrons in the two levels is different. Different lines of a multiplet show practically the same shift.

2) By assuming that an s-electron raises the level of the heavier isotope relative to the lighter isotope the sign of the field or volume shift is obtained.

3) The components of the even isotopes in a spectral line are always arranged in the order of the mass numbers A. The separations of the components are of the same order of magnitude but may show trends and abrupt changes. The ratios of the field or volume shifts between different isotopes are very nearly the same in different lines of the same element.

4) The lines of the odd isotopes or the centroids of their magnetic hyperfine structure patterns show a pronounced ''odd-even staggering'', that is, they do not lie midway between the adjacent even isotopes but are shifted towards the isotope with the lower A. Marked staggering has been observed in cadmium; extreme staggering, just reversing the order of the mass numbers, in tellurium; and an even greater effect has been demonstrated in barium.

In the study of the field or volume shift it is important to establish the contribution made to the overall isotope shift by the mass effect. The normal mass effect can always be calculated easily but the role played by the specific mass effect is generally extremely difficult to determine. However, a few rules-of-thumb can be stated (Kuhn[35]):

1) If lines of different multiplicity but of the same configuration show the same isotope shift, then the specific mass effect is not likely to be significant.

2) The isotope shift in a line due to the mass effect is proportional to $\frac{1}{A_1 A_2}$ where A_1 and A_2 are the mass numbers of the isotopes. If there are three isotopes A_1, A_2, A_3 and the measured ratio of the shifts differs appreciably from

$$\frac{\text{I.S. } (1,2)}{\text{I.S. } (2,3)} = \frac{A_3}{A_1}$$

and is found to be the same in different lines, the contribution of the mass effects can be assumed to be small.

Pauli and Peierls[41] were the first to suggest that a field dependent isotope shift could arise because the nucleus is not a point charge but has a finite volume within which there is a departure from the Coulomb potential "experienced" by the electrons. In this field or volume effect the departure from the Coulomb potential is least for the isotope with the smallest nuclear radius so that the term value of the smallest isotope lies "lowest" in the energy level diagram. Figure 2 shows the potential energy V between an electron and a nucleus as a function of their relative distance apart r, together with the corresponding energy level diagram. The figure shows the potential energies of two isotopes of mass numbers A and A + 1 with corresponding nuclear radii r_A and r_{A+1} where $r_{A+1} > r_A$. In general, if the nucleus is assumed to be spherical its radius r is given by

$$r = r_o A^{1/3} \qquad (1.48)$$

where $r_o = 1.2$ to 1.6×10^{-13} cm

The corresponding term values of the two isotopes are T_A and T_{A+1} while the term of a hypothetical point charge nucleus is T_c. ΔT_A and ΔT_{A+1}, the deviations of the terms

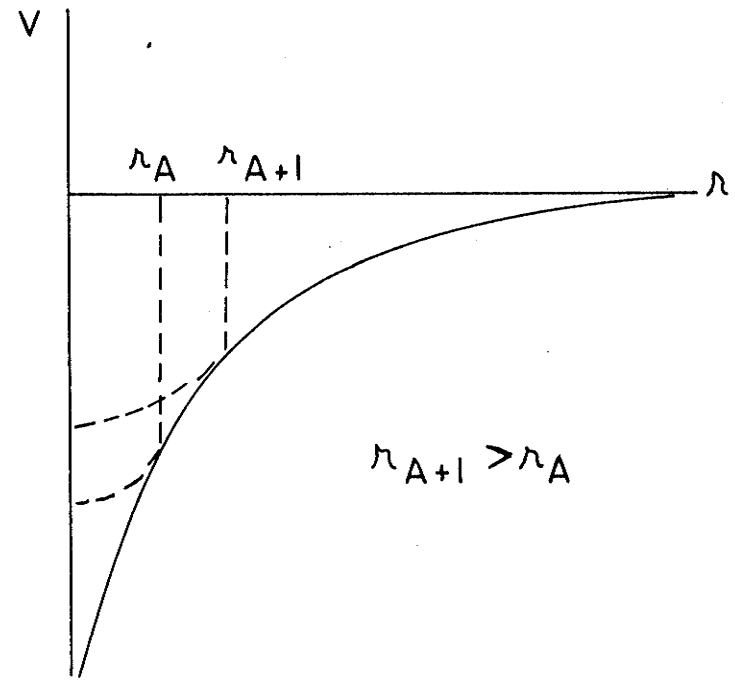

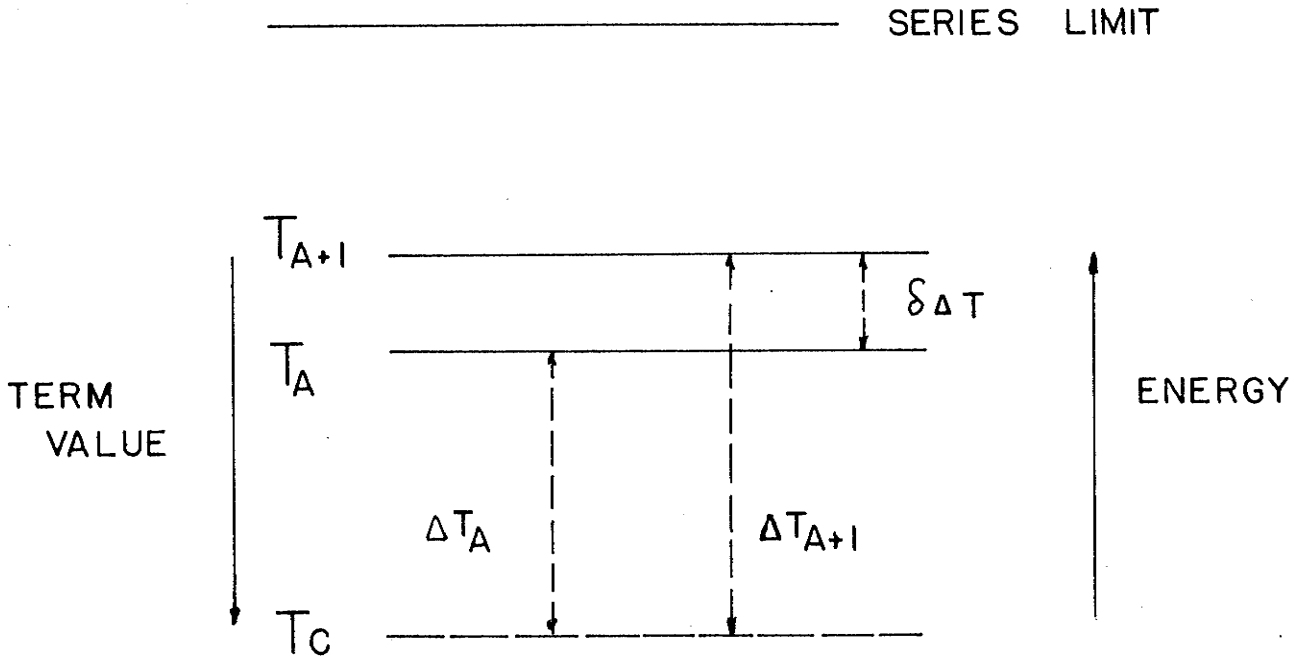

FIELD OR VOLUME EFFECT

FIGURE - 2

of the two isotopes from the term of a point charge nucleus, are the ''displacements'' in the term due to the nuclear field or volume effect, while the difference in the displacements, $\delta\Delta T$ is the isotope shift in the term due to the field or volume effect.

All the s electrons and to a much smaller extent all the $p_{1/2}$ electrons of the electronic configuration of a level contribute directly to the displacement of a term, while all the electrons of the configuration affect the displacement of the term indirectly through screening effects. However, this total displacement is not directly observable in practice. What is generally observed is the difference in energy between the components due to two different isotopes of the same element. This is the isotope shift in the spectral line. Since a spectral line involves a transition between two terms, the isotope shift in a spectral line will be equal to the difference in $\delta\Delta T$ between the two terms. Under favorable conditions the isotope shift minus the mass effect may be verynearly equal to the field dependent isotope shift due to a valence electron in only one of the terms. Thus in a transition of an electron from a p-state to an s-state the isotope shift minus the mass effect of the spectral line is very nearly equal to the field dependent isotope shift due to the s valence electron, where it is assumed that

the electronic cores of the two states are identical and that the smaller field dependent isotope shift of the p electron is negligible. Isotope shift studies are mostly restricted to spectral lines involving a transition to or from a term having one or two s electrons in the outermost shell.

The information about the size and angular shape of atomic nuclei which is obtained from the field or volume dependent isotope shift can be summarized in one number C_{exp}, the experimental isotope shift constant. C_{exp} is defined for two isotopes of the same element for a single valence s electron as

$$C_{exp} = \frac{\delta\Delta T_s}{\psi_s^2(0)\pi a_H^3/Z} = \frac{\delta\Delta T_s}{Z_o^2(1 - \frac{d\sigma}{dn})/n_o^3} \qquad (1.49)$$

where $\delta\Delta T_s$ is the field or volume dependent isotope shift in the term for two isotopes due to a single valence s electron.

$\psi_s(0)$ is the non-relativistic wave function of the s electron evaluated at the nucleus.

a_H is the Bohr radius.

Z is the atomic number of the element.

Z_o is the effective nuclear charge outside of closed electronic shells.

n_o is the effective principal quantum number and is equal to $n - \sigma$ where n is the principal quantum number and σ is the quantum defect.

$(1-\frac{d\sigma}{dn})$ is the Fermi-Segrè factor.

If the screening of the s valence electron on the electronic core is taken into account the above equation must be written as

$$\beta C_{exp} = \frac{\delta\Delta T_{exp}}{Z_o^{\,2}(1-\frac{d\sigma}{dn})/n_o^{\,3}} = \frac{\beta\delta\Delta T_s}{Z_o^{\,2}(1-\frac{d\sigma}{dn})/n_o^{\,3}} \qquad (1.50)$$

where β is a screening factor equal to $1 - \chi$ where $\delta\Delta T_{exp}$ is given by $(1-\chi)\delta\Delta T_s$. $\delta\Delta T_{exp}$ is the experimentally determined field or volume dependent isotope shift in the term due to the valence electron. The actual calculations of C_{exp} involve many difficulties and where they have been performed the accuracy is of the order of about 20%. In contrast, relative isotope shifts, can be determined more accurately and give C_{exp} on a relative scale[9,32,35]. Futhermore, the changes in these relative isotope shifts between successive pairs of isotopes, occurring either gradually or in ''jumps'', must be due to corresponding changes in the nuclear charge distribution resulting from the addition of neutrons to the nucleus, and therefore must give $\frac{\delta C_{exp}}{\delta N}$ on a relative scale to a considerable accuracy.

If C_{th} is the theoretical isotope shift constant for a pair of isotopes derived from a particular nuclear model, then a comparison of C_{exp} with C_{th} gives information about the validity of that particular nuclear model regarding

the change of nuclear charge distribution due to the addition of neutrons to the nucleus.

C_{th} has been calculated on the basis of a standard nuclear model of spherical, homogeneously charged, incompressible nuclei with radius r proportional to $A^{1/3}$. The isotope shift in a term due to the field or volume effect has been shown to be for an s electron

$$\delta\Delta T_s = \left|\Psi_s(o)\right|^2 \frac{\pi a_H^3}{Z} \; C_{th}\left(Z, r, \frac{\delta r}{r}\right) \qquad (1.51)$$

where $C_{th}\left(Z, r, \frac{\delta r}{r}\right) = \frac{12R_\infty(\rho+1)}{(2\rho+1)(2\rho+3)\Gamma^2(2\rho+1)} \left(\frac{2Zr}{a_H}\right)^{2\rho} \frac{\delta r}{r}$ (1.52)

in which $\rho = \sqrt{(1-\alpha^2 Z^2)}$ where α is the fine structure constant and Γ is the gamma function. (1.53)

Note that C_{th} depends on the properties of the two isotopic nuclei. Also note that in heavy atoms the Schrödinger wave functions must be replaced by Dirac functions. The theory implies that all transitions between levels of two given configurations should show almost the same isotope shift due to the field or volume effect. A comparison of the isotope shifts of two such transitions for which the specific mass effect should theoretically be different enables one to determine the relative importance of the two effects.

It is found that the values of βC_{exp} are in general smaller than C_{th} by a factor of between 1.5 and 7. Other evidence indicates that probably $\beta \approx 1$ so that this discrepancy cannot be accounted for by the screening effects of the electronic core[9,32]. Of the other factors which could possibly influence the isotope shift are the non-Coulombic interactions between the electrons and the neutrons, and the polarization of the nucleus by the orbital electrons, but these have been ruled out for various reasons[32,52]. Apart from this general discrepancy, a plot of $\beta C_{exp}/C_{th}$ against N brings out certain anomalies, and discontinuities at the ''magic'' neutron numbers N, which cannot be explained on the basis of this standard model. Furthermore, the ''staggering'' effect cannot be explained on this model.

In general, the smallness of the observed isotope shifts due to the field effect can be accounted for by nuclear compressibility and nuclear surface phenomena[52].

Brix and Kopfemann (1947) and Wilets, Hill and Ford (1953), have expressed the view that a large part of the field dependent isotope shift, especially most of its change with neutron number N and atomic number Z is related to an ''intrinsic quadrupole'' moment Q_o resulting from a nuclear deformation α. They assumed that even-even nuclei for which the spin I = 0 could have a charge distribution which deviates from spherical symmetry just like a nucleus

with $I \neq 0$. If $I = 0$ there is no preferred direction or ''axis of quantization'' so on averaging the charge distribution over all directions the deformation is detected as an increased volume effect rather than an observable quadrupole moment Q. On the basis of the dynamical model A. Bohr has derived the following relationship between Q and Q_o for strong coupling

$$Q = \frac{I(2I-1)}{(I+1)(2I+3)} Q_o \qquad (1.54)$$

where Q is the quantum mechanical quadrupole moment and is zero for $I = 0$ or $1/2$.

Q_o is the classical ''intrinsic'' quadrupole moment.

I is the nuclear spin.

The ''quadrupole'' isotope shift can be calculated if the deformed nucleus is approximated by a uniformly charged ellipsoid of revolution with the generating ellipse given by

$$r(\theta) = r'[1 + \alpha(3/2 \cos^2 \theta - \tfrac{1}{2})] \qquad (1.55)$$

where r' is the radius of the undeformed spherical nucleus of equal volume.

α is the deformation parameter and is equal to $2/3\,\varepsilon$ where ε is the ellipticity.

θ is the angle between the radius and the axis of symmetry.

For a prolate spheroid $\alpha > 0$ and for an oblate spheroid $\alpha < 0$. The calculation indicates that the shift in a term value as compared with its value for a spherical nucleus ΔT_α is given by

$$\Delta T_\alpha = |\Psi_s(0)|^2 \frac{\pi a_H^3}{Z} \times \frac{6R_\infty(\rho+1)}{5(2\rho+1)\Gamma^2(2\rho+1)} \left(\frac{2Zr}{a_H}\right)^{2\rho} \alpha^2 \qquad (1.56)$$

This relation has been shown to hold by A. Bohr if α describes the root mean square of the deformation due to a surface vibration rather than a static deformation. Experimentally what is observed is not ΔT_α but the change $\delta\Delta T_\alpha$ for a change in α at constant Z so that

$$\delta\Delta T_\alpha = |\Psi_s(0)|^2 \frac{\pi a_H^3}{Z} \times \frac{6R_\infty(\rho+1)}{5(2\rho+1)\Gamma^2(2\rho+1)} \left(\frac{2Zr}{a_H}\right)^{2\rho} \delta(\alpha^2) \qquad (1.57)$$

This together with the ''normal'' volume effect for a uniformily charged spherical nucleus $\delta\Delta T_s$ yields

$$\frac{\delta\Delta T_\alpha}{\delta\Delta T_s} = \frac{3}{10}(2\rho + 3) A \frac{\delta(\alpha^2)}{\delta A} \qquad (1.58)$$

Finally

$$\frac{C_\alpha}{C_{th}} = \frac{\delta\Delta T_\alpha}{\delta\Delta T_s} = \frac{5}{48} \frac{2\rho+3}{Z^2 r^4} A\delta(Q_o^2) [1-.36\pi Z a_H R_\infty] \qquad (1.59)$$

where the term in the bracket is a relativistic correction and where α has been expressed in terms of Q_o. The above expression is valid for two isotopes of even mass number differing by $\delta A = 2$. From the above relations we have

$$\frac{C_\alpha}{C_{th}} \propto \frac{\delta(\alpha^2)}{\delta N} \propto \frac{\delta(Q_o^2)}{\delta N} \tag{1.60}$$

and

$$\frac{\beta C_{exp}}{C_{th}} = \frac{C_\alpha}{C_{th}} + K \tag{1.61}$$

where the ''quadrupole'' effect has been added to the ''normal'' shift to give the total volume isotope shift. On the standard model $K = 1$ but if the compressibility of the nucleus is also considered $K \approx 0.7$.

The change in the relative isotope shift from isotope pair to isotope pair, which gives $\frac{\delta C_{exp}}{\delta N}$ on a relative scale, is then proprotional to $\frac{\delta C_\alpha}{\delta N} \propto \frac{\delta^2(\alpha^2)}{\delta N^2}$.

While the nuclear deformation affords a satisfactory explanation of the fluctuations of the isotope shifts and the discontinuities in the isotope shifts at the ''magic'' neutron numbers, it provides only a qualitative explanation of ''staggering''[32,52]. According to the theory of the ''quadrupole'' effect, the addition of a single neutron to a nucleus of even mass number leads to a smaller Q_o^2 and, hence, to a smaller isotope shift than the addition of two equivalent neutrons[32]. ''Odd-even staggering'' still presents a

challenging problem to nuclear theorists and it may be that several other effects, such as nuclear polarization contribute to it[32,52].

As has been mentioned screening effects influence the isotope shift and thereby introduce difficulties. While only s and to a lesser extent $p_{1/2}$ electrons contribute to the isotope shift directly, all electrons contribute indirectly through screening effects. At times this screening effect can be very large. For example in the HgI configuration $5d^{10}$ 6s6p the isotope shift is 261 x 10^{-3} cm.$^{-1}$ while in the HgII configuration $5d^{9}$6s6p the isotope shift is 350 x 10^{-3} cm^{-1}. The difference is ascribed to the screening effect of the additional 5d electron which causes the density distribution of the 6s electron to be shifted away from the nucleus. The isotope shift due to a ns^2 configuration is usually less than twice the isotope shift of an ns configuration because of screening. In an ns-np transition the isotope shift arises from the ns electron in the lower state. The ns electron causes a secondary effect through its screening part of the effective nuclear charge acting on the s electrons of the closed shells, causing them to expand and thus to reduce the isotope shift. Theoretical estimates of screening effects are difficult.

1.3 Magnetic Hyperfine Structure

Magnetic hyperfine structure is caused by the interaction of the nuclear magnetic moment with the valence electrons resulting in a splitting of the energy levels into a number of hyperfine structure states. The nuclear magnetic moment $\underline{\mu}_I$ arises from the orbital motion of the protons and the magnetic moments of the nucleons. The angular momentum of the nucleus can be represented by a dimensionless vector $\underline{I}$ which gives the angular momentum in units of $\hbar$. The maximum possible component of $\underline{I}$ in a fixed direction gives the nuclear spin I.

Then

$$\underline{\mu}_I = g_I \mu_N \underline{I} \qquad (1.62)$$

where g_I is the nuclear gyromagnetic ratio

μ_N is the nuclear magneton which is $\frac{\mu_o}{1833}$ where μ_o is the Bohr magneton.

Nuclear magnetic moments are usually expressed in units of nuclear magnetons in which case

$$\mu_I = g_I I \qquad (1.63)$$

μ_I is positive or negative depending upon whether $\underline{\mu}_I$ and $\underline{I}$ are parallel or antiparallel.

The magnetic field produced by an electron at the nucleus arises from the electron's orbital motion which is associated with its orbital angular momentum vector $\underline{\ell}$ and its intrinsic magnetic moment which is associated with its spin angular momentum vector $\underline{s}$.

The total angular momentum of the electron $\underline{j}$ is $\underline{\ell} + \underline{s}$. Where there are several electrons outside of closed shells, there may be LS coupling, jj coupling or some intermediate form of coupling between the valence electrons. The total angular momentum of the atom $\underline{F}$ is $\underline{I} + \underline{J}$. There are $2I + 1$ or $2J + 1$ magnetic hyperfine structure states depending upon whether $J \geq I$ or $I \geq J$. The statistical weight of a magnetic hyperfine structure state with quantum number F is $2F + 1$ so that the sum rule can be used to determine the intensity ratios of the components. The sum rule states that the sum of the intensities of all transitions originating or ending on a magnetic hyperfine structure state is proportional to the statistical weight of that state.

The interaction energy between the nuclear magnetic moment and the magnetic field due to the valence electrons for a given J level is

$$W(I,J) = \frac{1}{2} A_J[F(F + 1) - I(I + 1) - J(J + 1)] \tag{1.64}$$

while the separation between two magnetic hyperfine structure states ΔW of a given J level with quantum numbers F and F-1 is the product of the interval factor A_J and the higher F value,

$$\Delta W = A_J F \tag{1.65}$$

This is the interval rule.

For electron configurations with one electron outside of closed shells, the interval factor as determined by Goudsmit, Fermi and Segrè, Breit and Racah is, for a non-s electron

$$a_j = g_I \frac{\Delta\gamma_D}{Z_i} \frac{\ell(\ell+1)}{1836(\ell+1/2)j(j+1)} \frac{F_r(j,Z_i)}{H_r(\ell,Z_i)} \qquad (1.66)$$

and for an s electron

$$a_s = g_I \frac{8R_\infty \alpha^2 Z_i Z_o^2}{3n_o^3\ 1836}\left(1 - \frac{d\sigma}{dn}\right) F_r(j,Z_i) \qquad (1.67)$$

where a_j and a_s are the interval factors for a non-s and an s electron respectively in cm^{-1}.

g_I is the nuclear gyromagnetic ratio.

n_o is the effective principal quantum number.

Z_i is the effective nuclear charge in the inner region and is equal to Z for an s electron. For a p electron Z_i can be obtained from the doublet fine structure separation.

Z_o is the effective nuclear charge outside of closed shells and is 1 for a neutral atom and 2 for a singly ionized atom.

R_∞ is the Rydberg constant 109, 737.31 cm^{-1}.

α is the Sommerfeld fine structure constant $\frac{1}{137.04}$.

F_r and H_r are the relativistic corrections tabulated by Kopfermann[32].

n is the principal quantum number.

σ is the quantum defect and is equal to $n - n_o$

$\Delta\gamma_D$ is the interval in cm^{-1} between the two levels of the doublet with the same n and ℓ.

For electron configurations with more than one electron outside of closed shells, the various types of coupling must be taken into account in determining the interval factor. The vector model and the principle of energy sums enables explicit formulae to be derived for LS and jj coupling. For intermediate types of coupling quantum mechanics must be used. Breit and Wills have shown by an intermediate coupling calculation that the interval factors A for the triplet levels for a two electron configuration n s n ℓ are

$$A(^3L_{\ell+1}) = \frac{a_s}{2(\ell+1)} \quad \frac{2\ell+1}{2(\ell+1)} \; a_\ell + 1/2 \tag{1.68}$$

$$A(^3L_{\ell-1}) = -\frac{a_s}{2\ell} + \frac{2\ell+1}{2\ell} \; a_\ell - 1/2 \tag{1.69}$$

$$A(^3L_\ell) = \frac{1}{2\ell(\ell+1)} \Big\{ [(\ell+1)C_2^2 - \ell C_1^2] a_s$$

$$+(2\ell+3)C_1^2 a' + (2\ell-1)(\ell+1)C_2^2 a'' +$$

$$4C_1C_2 \sqrt{\ell(\ell+1)} \; a''' \Big\} \tag{1.70}$$

where a_s is the interval factor of the s electron.

a' and a'' are two splitting factors for the electron given by

$$\left.\begin{matrix} a' \\ a'' \end{matrix}\right\} = a_{\ell \pm 1/2} = \frac{\ell(\ell+1)}{j(J+1)} \frac{\Delta\gamma_M}{Z_i} \frac{1}{(\ell + 1/2)} \frac{g_I}{1836} \frac{F_r(j,Z_i)}{H_r(\ell,Z_i)} \tag{1.71}$$

a''' is a splitting factor designated by $a_{\ell + 1/2, \ell - 1/2}$ given by

$$a''' = \frac{1}{2(2\ell+1)(\ell + 1/2)} \frac{\Delta\gamma_M}{Z_i} \frac{g_I}{1836} \frac{G_r(\ell,Z_i)}{H_r(\ell,Z_i)} \tag{1.72}$$

where G_r is a relativity correction.

C_1 and C_2 are coupling coefficients which are

$$C_1 = \sin(\phi_o - \phi) \qquad C_2 = \cos(\phi_o - \phi) \tag{1.73}$$

$$\text{where } \phi_o = \tan^{-1} \sqrt{\frac{\ell}{\ell + 1}} \tag{1.74}$$

and where ϕ is a measure of the deviation from Russell-Saunders coupling and is given by

$$\sin^2 \phi = \frac{\Delta}{D} \tag{1.75}$$

Δ is the deviation of the term $^3L_\ell$ from its position in Russell-Saunders coupling where the interval rule is strictly obeyed.

D is the separation $^3L_\ell - {}^1L_\ell$

$\Delta\gamma_M$ is the fine structure multiplet splitting. For the singlet level, the intermediate coupling calculation yields an expression for the interval factor $A(^1L_\ell)$ similar to $A(^3L_\ell)$ but with C'_1 and C'_2 where $C_1 = -C'_2$ and $C_2 = C'_1$ substituted.

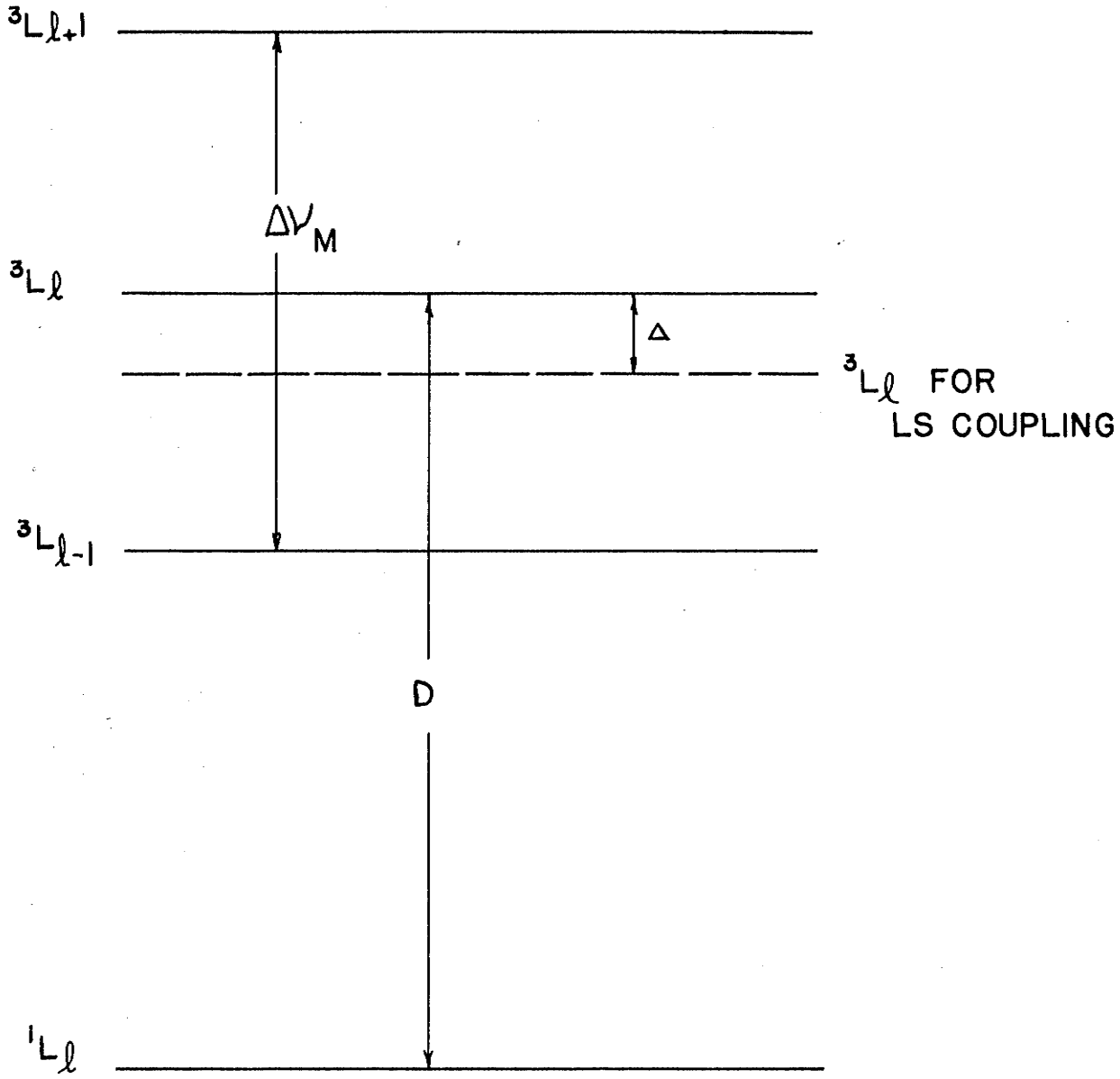

FINE STRUCTURE MULTIPLET OF TYPE

(sl) IN INTERMEDIATE COUPLING

FIGURE – 3

CHAPTER II

INTRODUCTION TO THE PROBLEMS

The research program consisted of two problems: a cadmium problem and a barium problem.

As mentioned in the first chapter it is experimentally possible to estimate the specific mass integrals K (ns, np) by comparing the isotopes shifts in the singlet and intercombination resonance lines of certain elements. Since isotope shifts in the CdI intercombination resonance line $\lambda 3261$ A^o ($5s^2\ {}^1S_o$ - $5s5p\ {}^3P_1$) had already been measured[29,47], it seemed a logical step to measure the CdI singlet resonance line $\lambda 2288$ A^o ($5s^2\ {}^1S_o$ - $5s5p\ {}^1P_1$) and thereby obtain an estimate of the specific mass integral K(5s, 5p).

Isotope shift studies in barium are of interest because the neutron shell closes at the magic number 82, because of the anomalous ''odd-even staggering'' reported by Arroe[2] and because of the apparently inconsistent results in the isotope shifts in BaI and BaII lines reported by the same author[2]. Isotope shift studies in barium have generated considerable interest in recent years. Measurements of isotope shifts in barium are difficult due to the large abundance of ${}_{56}Ba^{138}$ (71.7%) in natural barium and the smallness of the isotope shifts.

CHAPTER III

THE ATOMIC BEAM LIGHT SOURCE

3.1 Theory

A major problem in atomic spectroscopy is to obtain spectral lines with sufficiently narrow line widths so that the desired structure is not obscured. Every spectral line has a natural line width due to the uncertainty in the energy ΔE which arises from the finite lifetime Δt of an excited state. From Heisenberg's Uncertainty Principle ΔE and Δt are related as follows

$$\Delta E \cdot \Delta t \geq \frac{1}{2}\hbar \qquad (3.1)$$

Under ordinary circumstances the natural line widths of spectral lines are rarely larger than $0.001\ cm^{-1}$. In addition to natural line width, there are several other causes of line width which are summarized by Tolansky[48]. Among these are pressure broadening, resonance broadening, Zeeman and Stark broadening, and self-absorption broadening. However, the most important cause of line width in atomic spectroscopy is Doppler broadening which is due to the random thermal motion of the emitting atoms in the light source such that the atoms moving towards the observer emit a higher frequency than those receding from him. The Doppler half-width of a spectral line $\Delta\gamma$ is given by

$$\Delta\gamma = 2\sqrt{\log_e 2}\ \sqrt{2RT/Mc^2}\ \ \gamma\ \text{cm}^{-1} \qquad (3.2)$$

$$= 0.71 \times 10^{-6}\ \sqrt{T/M}\ \ \gamma\ \text{cm}^{-1}$$

where R is the gas constant.

T is the absolute temperature.

M is the molecular weight.

c is the velocity of light.

γ is the wave number of the radiation.

Doppler broadening can be reduced considerably by means of low temperature light sources and especially by means of an atomic beam light source. In an atomic beam light source the emitting atoms are made to travel perpendicularly to the direction of observation so that the average value of the component of velocity in the direction of observation is small. The atomic beam light source also reduces pressure broadening which is caused by collisions between the atoms.

The essential features of an atomic beam light source are given in Figure 4. An atomic beam light source consists of a high vacuum chamber divided into three sections, a furnace section for the evaporation of the material under study, a water cooled central section in which are mounted collimating slits, and an upper section in which the atoms are excited and from which the radiation is emitted. In the atomic beam light source used in this experiment, the evaporated atoms of cadmium or barium

moved from the furnace through the collimating slits to the upper chamber where they condensed on the liquid nitrogen trap. The atomic beam was excited by means of an electron beam passing perpendicularly to the atomic beam. The emitted light was observed perpendicularly to both the electron and atomic beams. In Figure 4, if O is the diameter of the oven aperture, S is the collimating slit length in the direction parallel to the line of sight, h is the distance between the oven slit and the trap, ℓ is the length of the spot collected on the liquid air trap, and d is the distance between the trap and collimating slit, then the largest deviation of the atomic paths from the axis of the beam is given by the angle α where

$$\alpha \approx \tan \alpha = \frac{\ell - S}{2d} = \frac{O + S}{2(h-d)} \qquad (3.3)$$

The collimation of the beam C is defined by[40]

$$C = \frac{1}{\alpha} \qquad (3.4)$$

The collimation of the atomic beam is then given by the geometry of the source as

$$C_{geom} = \frac{2(h - d)}{O + S} \qquad (3.5)$$

This can be checked experimentally by

$$C_{exp} = \frac{2d}{\ell - S} \qquad (3.6)$$

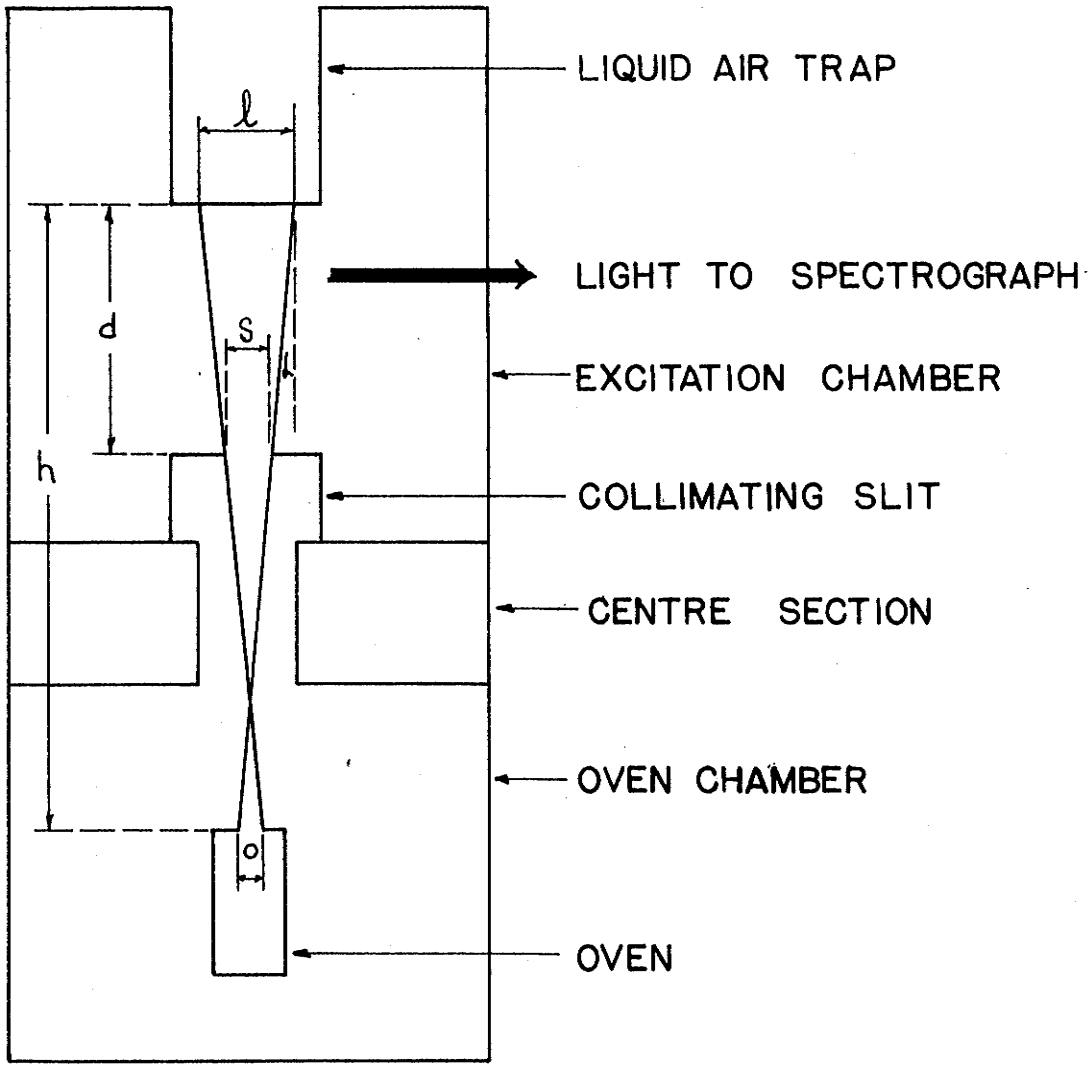

SCHEMATIC DIAGRAM OF AN ATOMIC BEAM LIGHT SOURCE

FIGURE - 4

The ratio of the half-widths of the spectral line from the beam to that from the vapor at the temperature of the oven is given by

$$\Delta\gamma_B/\Delta\gamma_o = 0.41/C \qquad (3.7)$$

The effective collimation depends also on the lens system used to focus the image of the source onto the slit of the spectrograph. If C' is the collimation of the light beam, then the effective collimation C_{eff} is given by

$$1/C_{eff} = 1/C + 1/C' \qquad (3.8)$$

If α' is the largest deviation of the light rays from the optical axis, then

$$C' = \frac{1}{\alpha'} \qquad (3.9)$$

3.2 Experimental Arrangement

The main features of the atomic beam light source used in these experiments are shown in Figure 5 and Plate 1. It is similar in construction to that described by Crawford et al[11,26,43].

The furnace section was pumped by a MC 275 oil diffusion pump in series with a Cenco Hypervac rotary forepump while the excitation chamber was pumped through a side arm by a pumping system consisting of a MCF 300 oil diffusion pump in series with a Cenco Megavac rotary forepump.

With this arrangement operating pressures in the range 10^{-5} to 10^{-6} mm. of Hg were obtained.

Two types of electrically heated furnace were used in the experiments. For the cadmium problem the furnace consisted of a steel core covered with ''Sauereisen'' cement in which was embedded the windings of no. 19 nickel-chrome wire. The furnace was fitted with a steel cover with a circular aperature. The furnace had a resistance of 8.5 ohms at room temperature. A plot of temperature against power input was obtained for the furnace with a chromel-alumel thermocouple. This type of furnace proved unsatisfactory for the study of barium as a temperature of about 1000°C was required to obtain a satisfactory barium beam whereas a temperature of only 400°C was required for a satisfactory cadmium beam. A second type of furnace was constructed for the barium experiments. It consisted of a steel core covered with a mixture of powdered alumina, aluminum nitrate and water in which was embedded the windings of 0.020 inch diameter tungsten wire.

The alumina and aluminum nitrate were mixed 3 parts to 1 with enough water added to make a paste. The covering was dried and then baked. The aluminum nitrate was reduced to aluminum oxide and acted as a binder. The furnace was fitted with a steel cover with a circular aperture. Furnaces of this construction would operate for about 10 hours before the barium would work its way into

the windings and cause a short circuit. These furnaces had resistances of about 1 ohm at room temperature. A plot of temperature against power input was obtained for the furnace operating in the vacuum by viewing the furnace with an optical pyrometer through a window in the vacuum chamber.

Best operating conditions for the electron gun had to be determined for each line examined. Operating conditions for a line not in the visible region of the spectrum were arrived at by comparing the intensities of photographic exposures of the line made under various operating conditions. Operating conditions for a line in the visible region of the spectrum were arrived at by the above technique and/or by simply viewing the beam directly or through filters. An attempt was made to keep the filament and grid currents low to minimize the heat produced and to avoid background light. The anode was water-cooled.

The beam was collimated sharply by a system of slits. This was evident from the clearly defined image on the liquid air trap and from the beam itself which appeared sharply defined in the region of the space charge when it emitted visible light.

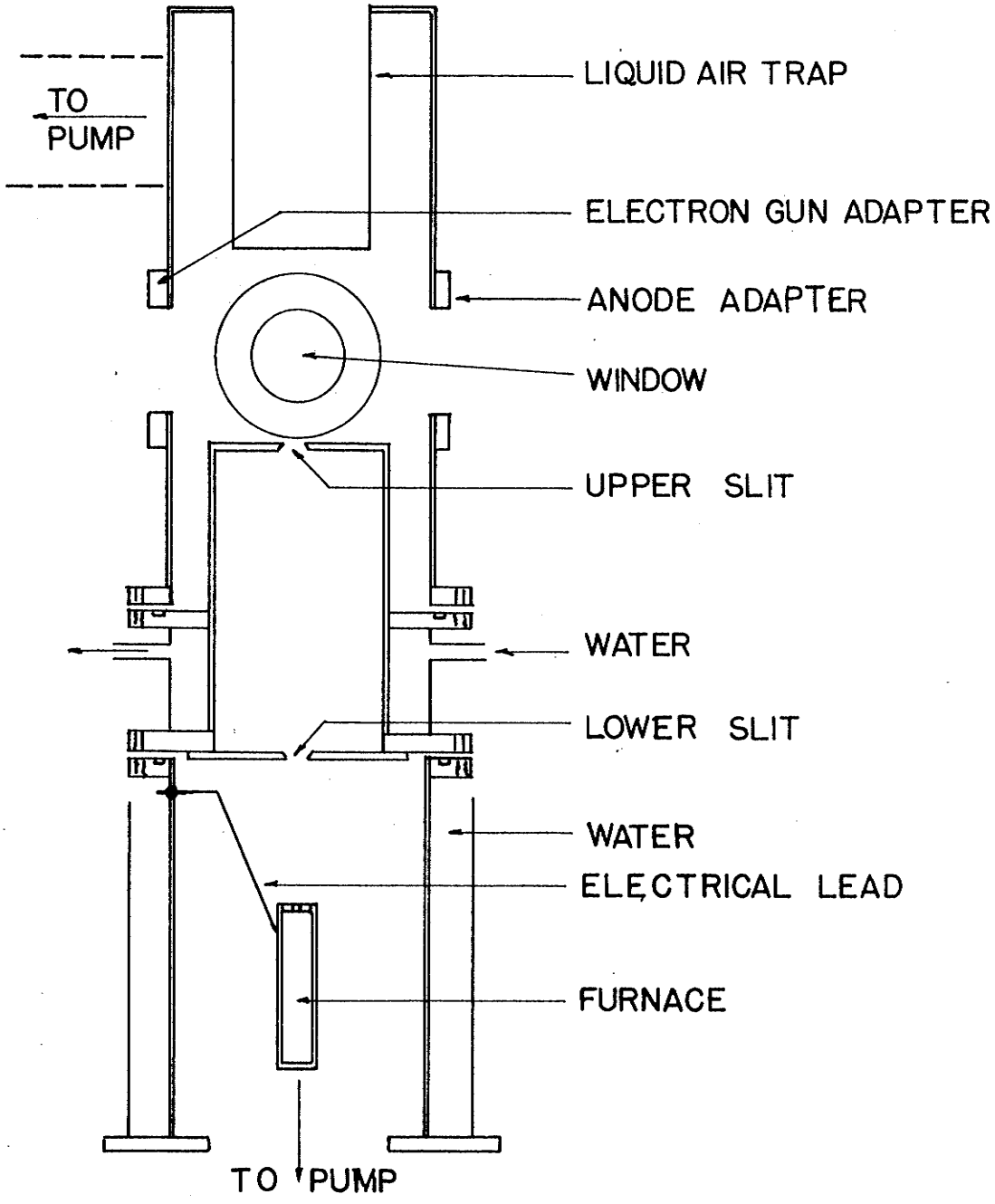

ATOMIC BEAM LIGHT SOURCE

FIGURE – 5

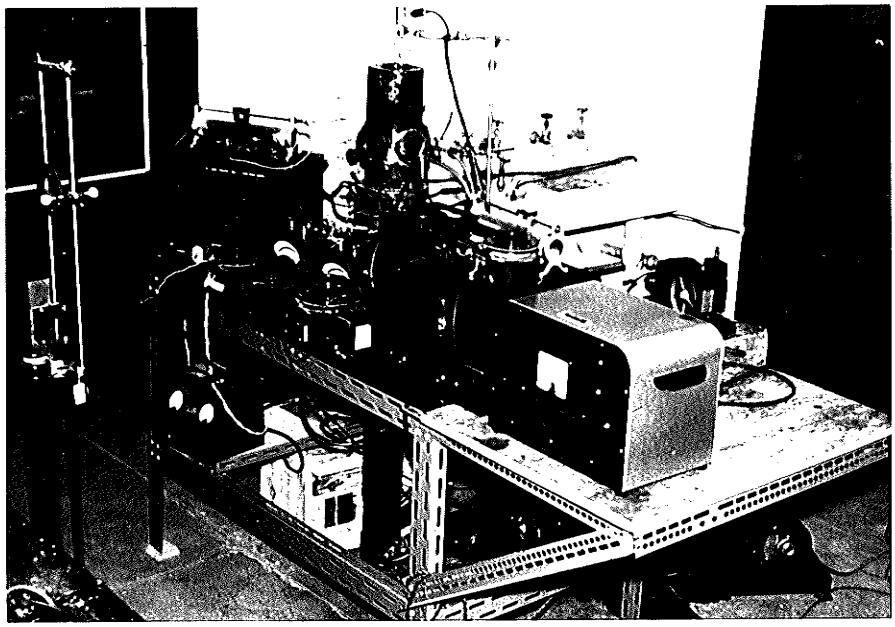

Plate 1: Atomic Beam Light Source

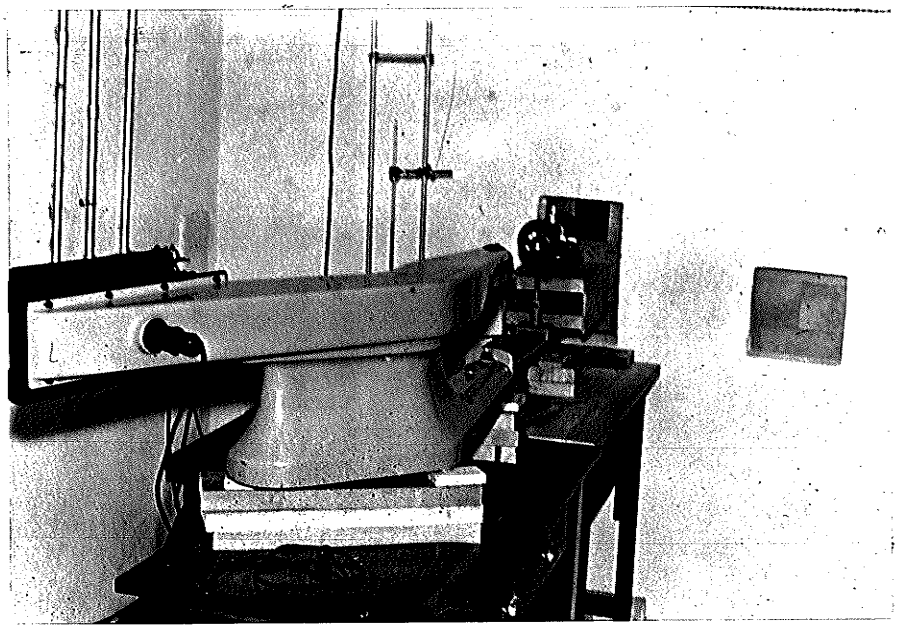

Plate 2: Optical Apparatus

CHAPTER IV

THE OPTICAL SYSTEM

4.1 Theory of the Fabry-Perot Interferometer

The Fabry-Perot interferometer is a high resolution instrument consisting of two parallel optical flats separated by a fixed spacer. The theory of the Fabry-Perot interferometer is discussed by Tolansky[48], Williams[53], and Kopfermann[32]. The essential results are summarized here.

Concentric interference fringes are formed at infinity and are given by the formula

$$n\lambda = 2\mu t \cos\theta \qquad (4.1)$$

where t is the separation of the partially reflecting coatings of the optical flats.

n is the order of the interference.

λ is the wavelength of the incident light.

μ is the refractive index of the medium between the optical flats.

θ is the semi-angle of the cone along whose surface the incident light travels.

If $d\gamma$ is the wave-number change corresponding to the change in order dn, then at or near the centre of the fringe system when moving from one fringe to the next in the adjacent order

$$\Delta\gamma = \frac{1}{2\mu t} \qquad (4.2)$$

where equation (4.1) has been differentiated and dn = 1 and cos θ = 1 have been substituted. By varying t the interorder separation can be varied at will. In air the interorder separation $\Delta\gamma$ is given by $\frac{1}{2t}$.

The intensity distribution in the fringes of a Fabry-Perot interferometer is given by Airy's formula

$$I = I_o \frac{T^2}{(1 - R)^2} \times \frac{1}{1 + \frac{4R}{(1 - R)^2} \sin^2 \delta/2} \qquad (4.3)$$

where I is the intensity

I_o is the intensity in the absence of the interferometer

δ is the phase difference between successive beams

R is the reflection coefficient
T is the transmission coefficient
A is the absorption coefficient

Furthermore

$$\delta = \left(\frac{2\pi}{\lambda} \right) 2\mu t \cos \theta \qquad (4.4)$$

and

$$R + T + A = 1 \qquad (4.5)$$

The ''half-width'' b of the fringe is

$$b = \frac{2}{\pi} \sin^{-1} \frac{1 - R}{2\sqrt{R}} \approx \frac{1 - R}{\pi \sqrt{R}} \qquad (4.6)$$

The theoretical ''instrumental width'' $\delta\gamma$ of the interferometer is

$$\delta\gamma = b\Delta\gamma \approx \frac{1 - R}{2\pi t \sqrt{R}} \qquad (4.7)$$

The theoretical resolving power A of the interferometer is

$$A = \frac{\gamma}{\delta\gamma} = \frac{n}{b} \approx \frac{2t}{\lambda b} \tag{4.8}$$

As the theoretical resolving power contains λ it is usual to speak of the theoretical resolving limit $\underline{d\gamma}$ of the Fabry-Perot interferometer which is defined as

$$\underline{d\gamma} \approx \frac{1}{2t}\,\frac{1}{N} \tag{4.9}$$

where N is the ''effective number of interfering component beams'' and is given by

$$N = \frac{1}{b} \approx \frac{\pi\sqrt{R}}{1 - R} \tag{4.10}$$

It is clear from equation (4.7) and (4.9) that $\delta\gamma$ and $\underline{d\gamma}$ are equal.

Airy's formula was derived assuming a monochromatic light source; reflecting planes infinite in extent, exactly parallel, and perfectly plane; and neglecting the small influence of the optical flats on the reflection and absorption coefficients. As these conditions are not met in practice, the theoretical ''instrumental width'' and hence the theoretical resolving limit can only serve as a lower limit. To find the actual ''instrumental half-width'', the fringes must be photo-

metered. Kuhn[38] reports that the smallest fraction of an order which has been resolved in the red region with silver films is 1/50, while the smallest fraction of an order which has been resolved in the near ultra-violet region with aluminum films is 1/15.

4.2 Experimental Arrangement

The spectral lines under investigation were in the ultraviolet and visible regions of the spectrum. All optical apparatus was of quartz. A Hilger Medium Quartz Spectrograph (f/10) was used to isolate the particular line under study from the other spectral lines. The high resolution was supplied by a Fabry-Perot interferometer. The plates and spacers were of fused silica. The plates were coated with spectroscopically pure aluminum by vacuum evaporation if the line under study was in the ultraviolet region or with silver if the line was in the visible. The Fabry-Perot interferometer was mounted externally to the spectrograph. Plate 2 is a photograph of the optical apparatus.

Two quartz lenses were also used in the optical arrangement. The focal lengths of the two lenses were 107.5 cm and 53.5 cm in the visible. Using the ''lensmaker's equation'' for a thin lens in air,

$$1/f = (n - 1)\, K \qquad (4.11)$$

(where f is the focal length of the lens

n is the refractive index of the material of the lens

K is a constant depending upon the radii of curvature of the lens),

and the indices of refraction of quartz in the visible (λ5500 A^{o}) and at the wavelength under study, the focal lengths of the lenses at the wavelength of the line under study were estimated. The 107.5 cm lens was placed so that the excited part of the atomic beam was at the focal point of the lens so that parallel light beams entered the interferometer. The Fabry-Perot fringes were focused on the slit of the spectrograph by the high quality 53.5 cm lens. The final focussing of this lens for each wavelength under study was made by photographing the very fine off-center fringes for a series of 1 mm positions of the lens, and then selecting the lens position which corresponded to the exposure with the sharpest fringes.

The atomic beam source was carefully positioned on the axis of the spectrograph. The two lenses were then properly positioned. Finally the axis of the interferometer was aligned by viewing the fringe system through the spectrograph.

The interferometer plates were adjusted for parallelism by observing the fringes of the mercury green line. The light source was a water-cooled Hg^{198} discharge

which produces lines with a small half-width. The green line was isolated with a Wratten No. 77 filter.

The quartz plates of the interferometer were coated with a film of spectroscopically pure aluminum or with a film of silver in an evaporator constructed for this purpose and described by Sutherland[46]. Evaporation pressures of the order of 10^{-5} mm of Hg were obtained in all cases. To obtain aluminum films of good quality the plates must be coated in a single evaporation. The time of evaporation was selected from a curve of transmission in the blue vs time of evaporation which had been prepared previously. The transmissions in the blue were measured with a commercial light meter and a blue filter in conjunction with a white light source. From the curves of Burridge et al[10] the reflection coefficient R could be determined for a particular wavelength in the ultraviolet. Silver films of good optical quality could be obtained by a series of evaporations. Hence when the interferometer plates were to be coated with silver films the apparatus for determining transmissions in the blue was mounted directly on the evaporator. The transmission was measured after each evaporation and the process continued until the desired transmission was obtained. The reflection coefficient R at the particular wavelength under study was estimated from the curves of Kuhn and Wilson[36]. The quantity pt, where p is in units of 10^{-5} mm of Hg and t is in

minutes, gives a measure of the optical quality of the films. The lower the value of pt, the lower is the probability of an impurity atom striking the plates during the evaporation. However, in order to evaporate in a shorter time a higher current must be used thus increasing the probability of releasing absorbed gases from the vacuum chamber. Films of optimun quality are produced if a proper balance is obtained between these two effects. It has been shown that if $pt < 3$, aluminum films are of good optical quality[36]. It is assumed that if pt is also small silver films are of good optical quality.

Temperature and pressure variations cause displacements of the fringe system through variations of μ in equation (4.1). The interferometer and spectrograph were accordingly housed in a separate room where the temperature variation was controlled [illegible] by means of an ether mercury thermostat[17] with an electronic relay connected to several electric heaters mounted on the walls of the room. The refractive index of air under ordinary conditions is about 1.0003 and μ-1 is proportional to the density of the air, so that a change in pressure Δp causes a shift in the interference pattern $\Delta\gamma$ given by

$$\Delta\gamma = 0.0003 \left(\frac{\Delta p}{p} \right) \gamma \text{ cm}^{-1} \qquad (4.12)$$

A rise in pressure of 1 mm has the same effect as a drop of 0.36°C in the temperature[48]. The pressure and temperature must be so controlled that any broadening does not mask the structure which is sought nor introduce an appreciable error through broadening. The temperature in the room was so controlled that the change in temperature of the interferometer was 0.01°C (which corresponds to a change in pressure of less than 0.03 mm of Hg) while the exposures were taken so that the pressure did not fluctuate by much more than 0.1 or 0.2 mm of Hg. Taking $p \sim 70$ cm, $\Delta p =$ .2 mm Hg and $\lambda = 2288$ A° (the shortest wavelength of the lines studied) the shift of the fringes from equation (4.12) is

$$\Delta\gamma = 0.0027 \text{ cm}^{-1}$$

If the temperature effect is taken into account the total shift is around 0.003 cm^{-1} which is smaller than any of the separations measured. It should be noted that the case considered here is the worst possible one. The fringe shift due to pressure and temperature fluctuations is certainly much smaller than this in practice.

CHAPTER V

THE CADMIUM PROBLEM

5.1 Discussion of the Problem

There are eight naturally occurring isotopes of cadmium, six even and two odd. Their relative abundances are given in Table 1 (from Bainbridge and Nier[4]).

Table 1: Relative Abudances of the Isotopes of Natural Cadmium.

Isotope	106	108	110	111	112	113	114	116
%	1.22	0.88	12.4	12.8	24.1	12.3	28.8	7.6

Each even isotope of cadmium has a zero nuclear spin. The odd isotopes have a spin of 1/2 and a negative magnetic moment.

As already mentioned, an experimental estimation of the specific mass effect can be made by comparing the isotope shifts in a pair of lines. Such a pair is the singlet and intercombination resonance lines of cadmium. The singlet resonance line $\lambda 2288$ A^{o} ($5s^2\ {}^1S_o$ - $5s5p\ {}^1P_1$) and the intercombination resonance line $\lambda 3261$ A^{o} ($5s^2\ {}^1S_o$ - $5s5p\ {}^3P_1$) have a common lower level. The upper levels arise from the same 5s5p electronic configuration. See Figure 6. The field effect shift of either a $p_{1/2}$ or a

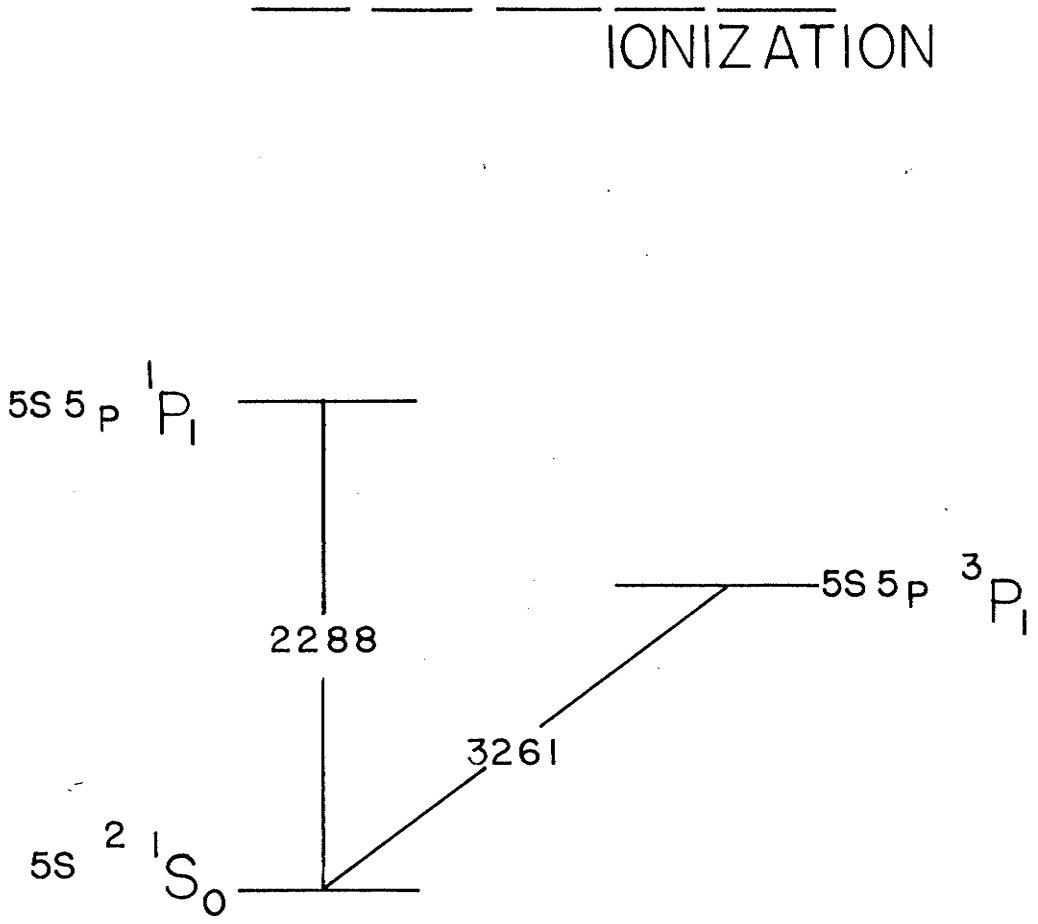

CdI RESONANCE LINES

FIGURE - 6

$p_{3/2}$ electron is small compared to the shift due to an s electron so that the shift arising from the field effect should be the same in both of these lines. The specific mass effect, predicts that the shifts of these two lines should differ by an amount depending upon the specific mass integral K(5s,5p) .

The shifts observed in λ2288 A^o are reported here, and are compared with the shifts in λ3261 A^o which were reported earlier by Kelly and Tomchuk[29,47]. The results obtained here are then compared with similar results in the lighter elements obtained by Crawford et al[12] for zinc, by Kelly[27] for magnesium and by Hughes[21] for strontium.

5.2 Experimental Considerations

The singlet resonance line was excited in the atomic beam source previously described. The collimation of the beam was such that the source line width was estimated to be 0.002 cm^{-1}. The general features of the optical apparatus have already been described. The Hilger medium quartz spectrograph isolated λ2288 A^o from the other spectral lines while the Fabry-Perot interferometer which was mounted externally to the spectrograph supplied the high resolution needed for resolving the closely spaced components of λ2288 A^o. A 10 cm spacer was used. The reflectivity of the aluminum films at λ2288 A^o was estimated to be 80% from the measured transmission coefficient

in the blue and the curves of Burridge, Kuhn and Pery[10] so that about $\frac{1}{15}$th of an order could be resolved. The patterns were recorded on Ilford QI and QII plates with exposure times up to two hours.

5.3 λ2288 A° Results

The line λ2288 was resolved into three closely spaced components; two of nearly equal intensity and a third of lower intensity. Twenty-five exposures with structure in two to five orders were measured five times by each of two observers. Microphotometer measurements were not satisfactory due to the curvature of the fringes. The three components are designated A, B and C with A having the highest frequency. A photograph of the fringes appears in Plate 3. The measured separations are

$$\Delta\gamma(A,B) = 16.8 \pm 0.3 \times 10^{-3} \text{ cm}^{-1}$$

$$\Delta\gamma(B,C) = 12.5 \pm 0.5 \times 10^{-3} \text{ cm}^{-1}$$

The errors quoted are the probable errors determined from the mean deviations. The assignment of component A to a blend of components due to isotopes 110 and 111, component B to a blend of components due to isotopes 112 and 113 and C to isotope 114 is consistent with visually estimated relative intensities. This is illustrated in Figure 7.

Plate 3: CdI λ2288 A^{O} Structure

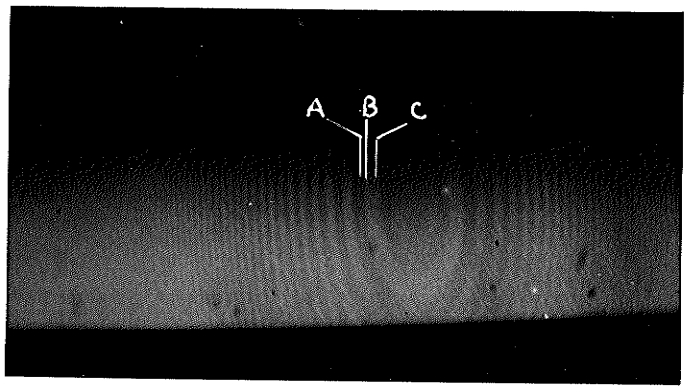

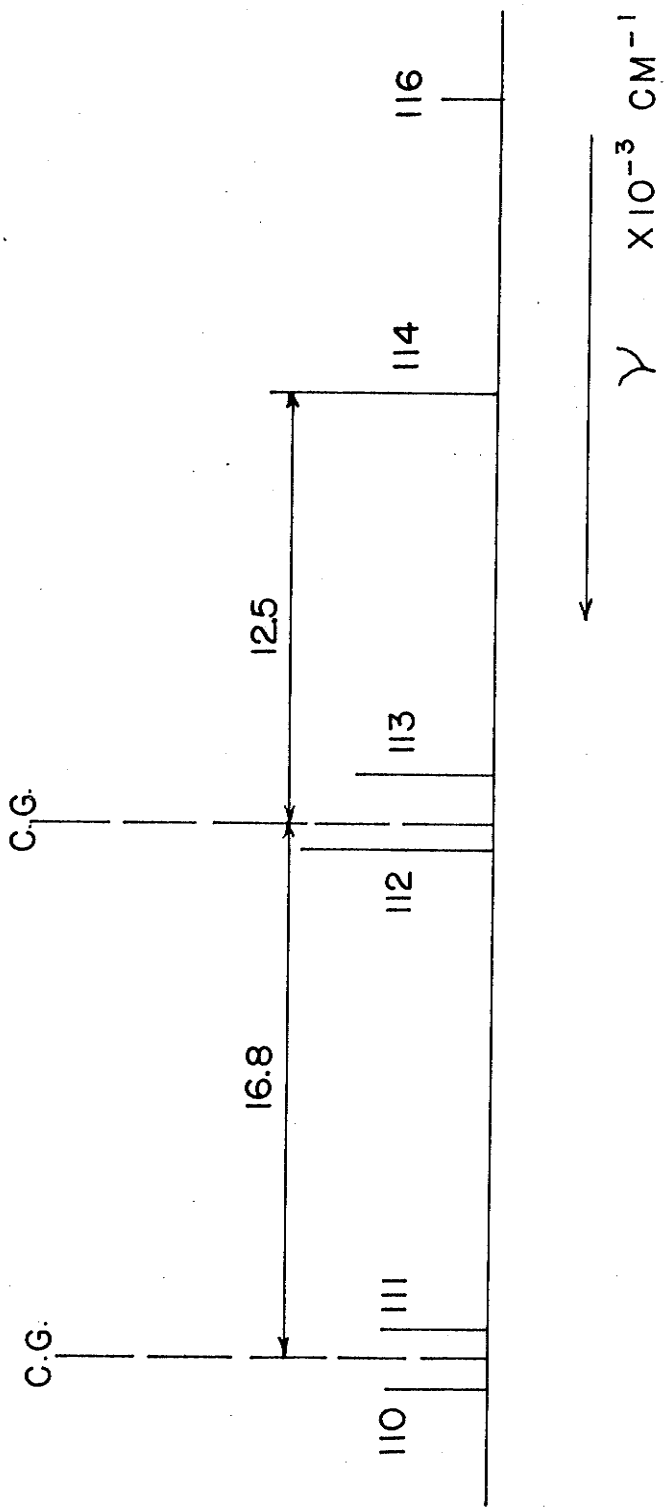

ISOTOPE SHIFTS IN CdI λ 2288 Å

FIGURE – 7

The unresolved separations of the isotope pairs (110-111) and (112-113) were assumed to be in the ratio found in λ3261 A°, and, by Kuhn and Ramsden[37] in λ4416 A°. Using the relative abundance as a weight factor and assuming that the magnetic hyperfine structure in the $^1P_1$ level is negligible*, the separations between the even isotopes were calculated to be

$$\Delta\gamma(110,\ 112) = -17.0 \pm 0.6 \times 10^{-3}\ \text{cm}^{-1}$$

$$\Delta\gamma(112,\ 114) = -13.2 \pm 1.0 \times 10^{-3}\ \text{cm}^{-1}$$

The negative sign means that the lighter isotope has the higher frequency. The error has been doubled to allow for the extra uncertainties introduced in making the calculations. A plot of theoretical intensity curves shows that the influence of the isotope 116 on the position of 114 is much less than the experimental error.

5.4 λ3261 A° Results

The isotope shifts in the CdI intercombination resonance line λ3261 A° ($5s^2\ ^1S_0$ - $5s5p\ ^3P_1$) were measured previously by Kelly and Tomchuk[29,47], for seven of the eight naturally occurring isotopes of cadmium using an atomic beam light source together with a Fabry-Perot interferometer. The measured shifts are given in Table 2 and Figure 8.

* An intermediate coupling calculation shows that the $^1P_1$ level consists of two magnetic hyperfine structure states with a separation of about 5 mK. This separation could not be detected experimentally and consequently the assumption is justified.

Table 2: Isotope Shifts in CdI λ3261 A^{o}

Isotope Pair	Isotope Shift ($\times 10^{-3}$ cm^{-1})
116, 114	9.3 ± 0.4
114, 112	13.5 ± 0.4
113, 112	2.6 ± 1.5
112, 110	16.3 ± 0.5
111, 110	1.9 ± 1.6
110, 106	35.4 ± 2.2

The position of 108 was not determined because of its low percentage abundance.

Since each odd isotope has a spin of 1/2 each odd isotope gives rise to two magnetic hyperfine structure components in the CdI intercombination resonance line λ3261 A^{o}. Since both magnetic moments are negative the splitting of the $^{3}P_{1}$ level places the weaker component on the high frequency side of the stronger component. The isotope shift of each odd isotope is for the calculated position of the centroid of its magnetic hyperfine structure components. The errors quote in Table 2 are the estimated probable errors from the mean deviations.

The isotope shifts of the even isotopes decrease with increasing mass number while the odd isotopes show a pronounced even-odd staggering (Z = 48 for cadmium), that is, the centroids of the odd isotopes lie closer to the next even isotope with the smaller mass number.

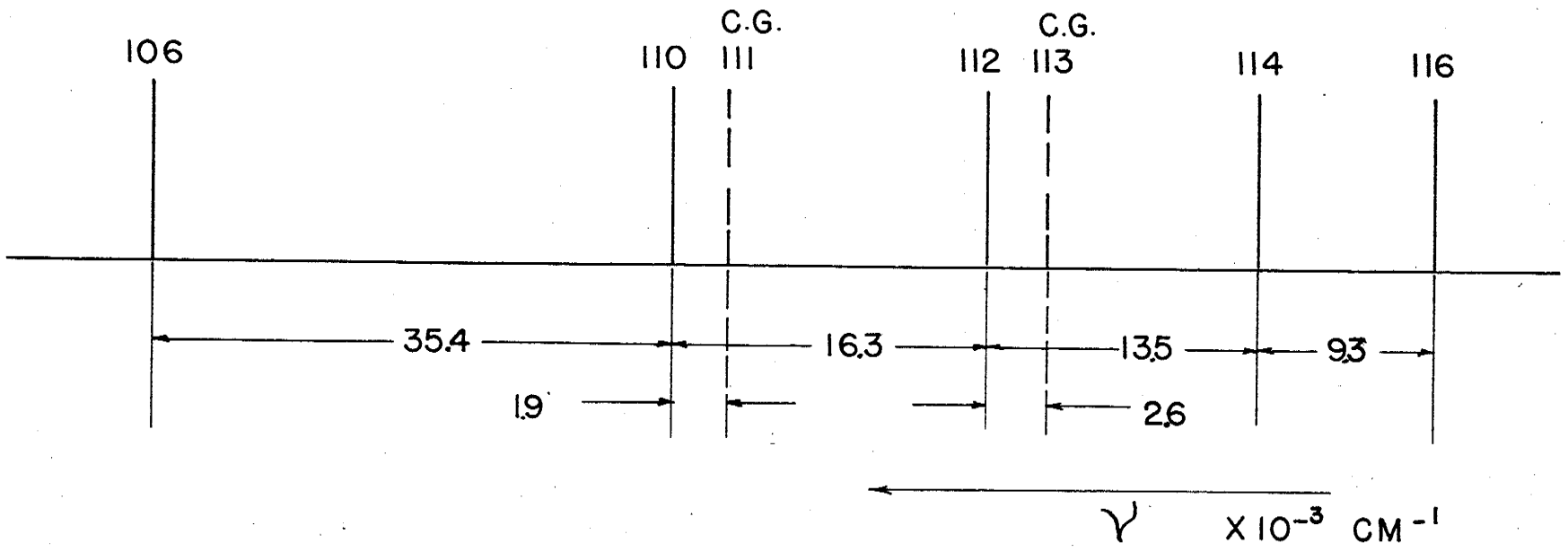

ISOTOPE SHIFTS IN CdI λ 3261Å

FIGURE – 8

When the normal mass effect was taken into account the ratios of these isotope shifts were found to be in good agreement with the corresponding ratios determined by Kuhn and Ramsden[37] for the CdII line λ4416 A° indicating that any residual specific mass effect is quite small.

5.5 Discussion of Results and Conclusions

The isotope shifts between even isotopes in the singlet (λ2288 A°) and the intercombination (λ3261 A°) resonance lines may be analysed in a manner similar to that used for the ZnI resonance lines (Crawford et al[12]).

Table 3: Isotope Shift in CdI (in 10^{-3} cm^{-1})

	2288 A°		3261 A°	
	110-112	112-114	110-112	112-114
Observed shift	-17.0	-13.2	-16.3	-13.5
Normal shift	+ 3.9	+ 3.7	+ 2.7	+ 2.6
Residual shift	-20.9	-16.9	-19.0	-16.1
3261-2288($\delta\Delta\gamma$)			+ 1.9	+ 0.8

The residual shift $\Delta\gamma$ is the observed shift minus the normal mass shift. The differences between the residual shifts are +1.9 ± 1.1 for (110-112) and +0.8 ± 1.4 (112-114). These two values agree within experimental error and the average is +1.3 ± 1.3.

From the specific mass theory the difference between the intercombination and singlet resonance lines is

$$\delta\Delta\gamma = -4\, R_{\infty}\, m \left\{ \frac{1}{M_1} - \frac{1}{M_2} \right\} K\,(ns,\ np)$$

The data for Mg (Kelly[27]), Zn (Crawford et al[12], Hately and Littlefield[18]), Sr (Hughes[21]) and Cd for the shifts arising from isotopes differing by two neutrons are summarized in Table 4.

Table 4: Specific Mass Effect Integrals

n	$\delta\Delta\gamma$ ($\times 10^{-3}$ cm^{-1})	K(ns, np)
Mg 3	+57.9 ± 1.6	-0.076 ± 0.002
Zn 4	+10 ± 1.5	-0.091 ± 0.014
Sr 5	+ 5.6 ± 1.8	-0.033 ± 0.024
Cd 5	+ 1.3 ± 1.3	-0.03 ± 0.03

The value of the specific mass integral K(ns, np) is not very sensitive to the value of the principal quantum number n, and for n = 5 appears to be decreasing. The factor $\frac{\Delta M}{M_1\, M_2}$ in the heavy elements will reduce the resulting specific mass shifts to small values. Consequently in the heavy elements one can expect to obtain specifically nuclear data from the observed shifts.

CHAPTER VI

THE BARIUM PROBLEM

6.1 Discussion of the Problem

Barium has seven stable isotopes whose relative abundances are listed in Table 5 (from Bainbridge and Nier[4]).

Table 5: Relative Abundances of the Isotopes of Natural Barium

Isotope	138	137	136	135	134	132	130
% Abundance	71.7	11.3	7.8	6.6	2.4	.096	.103

Isotope shift studies of barium are of interest because of the proximity of the magic neutron number 82 (Z = 56 for barium) and because of the anomalous and inconsistent shifts reported by other investigators.

There have been a number of experiments to determine isotope shifts in the BaI singlet resonance line $\lambda 5535$ A^{o} ($6s^2\ {}^1S_o$ - $6s6p\ {}^1P_1$). Kopfermann and Wessel[33,34] first used an atomic beam to absorb the line $\lambda 5535$ A^{o} and later used an atomic beam excited by resonance fluorescence. They observed no clear resolution of components and interpreted the wing on the high frequency side of the main component to be due to isotope shift alone - the magnetic hfs splitting of the components due to the odd isotopes being assumed small compared with the isotope shifts. Their interpretation of the structure is summarized in Table 6.

The weak component at +24 mK is supported by inconclusive absorption data only and may be neglected.

This line was further investigated by Arroe[2] who used a hollow cathode light source cooled with liquid air and containing samples of either natural barium or barium samples enriched in one of the less abundant isotopes. The wavelengths of the light emitted by the various samples were then compared by means of a Fabry-Perot interferometer with plate separations between 1 and 4 cms. The isotopes shifts derived by Arroe are given in Table 7. They differ markedly from the data of Kopfermann and Wessel.

Arroe also studied the structure of the resonance lines of the BaII lines λ4934 A^{o} and λ4554 A^{o} ($6s\ ^{2}S_{1/2}$-$6p\ ^{2}P_{1/2,3/2}$) using the same method. In these lines the magnetic hyperfine structure of the odd isotopes is large and the centroids must be calculated. Each odd isotope has a spin of 3/2 and a positive nuclear magnetic moment. The resulting isotope shifts are given in Table 8. These isotope shifts are larger than those observed in the arc line and the order of the isotopes is different as indicated in Table 9. Interpretation of the results in terms of a nuclear volume effect (Kopfermann[32]) is difficult as neither the order of the isotopes found in BaI and BaII nor

the ratios giving the relative shifts between the isotopes are the same.

Unpublished results on the structure of λ5535 A^{o} were obtained by Crawford et al[13] who employed an atomic beam in emission. This group found a strong component and satellites at +9.7 and +17.2 mK. The intensity ratios were found to be 72:14:6. These results are in rough agreement with those of Kopfermann and Wessel.

Crawford's group also studied the structure of the BaII resonance line λ4554 A^{o}. The resolution of the magnetic hyperfine structure was not complete and Arroe's value for the splittings of the $^{2}S_{1/2}$ level were used to calculate the centroids of the odd isotopes. A wing on the high frequency side of the strong component was assigned to 136. The centroids of 137, 136 and 135 were found to be at +13, +9 and +19 mK relative to 138. These investigators did not take 134 into consideration.

An investigation by Jackson (1957)[22] used the absorption of the resonance line in three atomic beams each with a high collimation ratio of 28:1. Jackson observed components at 0.0, +3.8, +9.9 and +18.4 mk with intensities 20:4.5:2.5:1. In order to fit the observed spacings and intensities Jackson assigned a magnetic hyperfine structure splitting to the $^{1}P_{1}$ level of the two odd isotopes but used a positive A-factor for the magnetic structure.

Mack[39], in an attempt to resolve the inconsistencies in the data for λ5535 A°, used a negative A-factor, as predicted by the theory of Breit and Wills[8], for the magnetic hyperfine structure of the $^1P_1$ levels of the odd isotopes. The wide structure observed by the atomic beam methods was explained by the magnetic hyperfine structure of the odd isotopes and the small isotopes shifts found by Arroe were preserved, except for a rearrangement of the order of the isotopes. Mack's order of the isotopes is the same as that observed by Arroe in BaII. Mack was unable to reconcile his pattern completely with observed intensities.

During the progress of our experiments further atomic beam results were obtained (Jackson, 1961[23]) and two further studies using enriched isotopes were made (Razumovskii and Chaika[42], and Jackson and Duong 1963a[24]). The results of these experiments are given in Tables 6, and 7. The order of the isotopes in all experiments with enriched isotopes in λ5535 A° is the same although there are differences in the observed magnitudes. The order of isotopes in λ5535 A° is different from the order in Arroe's BaII results. The isotopic orders in the various experiments are given in Table 9.

A further experiment by Jackson and Duong (1963b)[25] employed an atomic beam of enriched odd isotopes to absorb λ5535 A° within a spherical Fabry-Perot interferometer.

This experiment gives accurate values of the magnetic hyperfine splitting factors, A, and the quadrupole-moment coupling factors, B, for both odd isotopes and places the positions of the isotopes 137 and 135 at +7.0 ± 0.3 and +8.1 ± 0.3 mK relative to 138.

Table 6:

Atomic Beam Observations of BaI λ5535 ($6s^2\ ^1S_o$ - $6s6p\ ^1P_1$)

(The strongest component is taken as zero. In mK, 1 mK = 10^{-3} cm^{-1}.)

Kopfermann and Wessel	0	-	+7	+12	+18	+24
Crawford et al	0	-	-	+9.7	+17.2	-
Jackson (1957)	0	-	+3.8	+9.9	+18.4	-
Jackson (1961)	0	+2.0	+3.9	+9.1	+18.1	-
Kelly and Tomchuk	0	-	+4.4	+10.0	+18.7	-

Table 7:

Isotope Shift in BaI (mK)

$\lambda 5535$ ($6s^2\ ^1S_0$ - $6s6p\ ^1P_1$)

Isotope	138	137	136	135	134	132	130
Arroe	0	+5.2	+2.2	+7.4	+4.4		
Jackson (1957)	0	+4.9	+4.2	+14.5	+8.0		
Mack	0	+4.7	+3	+6.7	+5		
Razumovskii and Chaika	0	+5.7	+4.2	+7.6	+4.7		
Jackson and Duong (1963a)	0	+7.7	+4.2	+8.4	+4.6	+7.4	+7.8
Jackson and Duong (1963b)	0	+7.0	-	+8.1	-		

Table 8:

Isotope Shift in BaII (mK)

$\lambda 4934$ ($6s\ ^2S_{1/2}$ - $6p\ ^2P_{1/2}$)

$\lambda 4554$ ($6s\ ^2S_{1/2}$ - $6p\ ^2P_{3/2}$)

Isotope	138	137	136	135	134
Arroe $\lambda 4934$	0	+6.0	+4.8	+11.1	+9.6
Arroe $\lambda 4554$	0	+6.4	+5.4	+12.6	+10.8
Crawford et al $\lambda 4554$	0	+13	+9	+19	
Kelly and Tomchuk $\lambda 4934$	0	+10.1	+6.7	+13.0	+8.7
Kelly and Tomchuk $\lambda 4554$ (3cm spacer)	0	+9.8	+7.2	+13.1	+9.6
(5cm spacer)	0	+9.3	+7.2	+12.6	+9.6

Table 9:

Order of the Isotopes

Isotope	138	137	136	135	134
Arroe BaI	1	4	2	5	3
Arroe BaII	1	3	2	5	4
Crawford et al BaII	1	3	2	4	-
Jackson (1957) BaI	1	3	2	5	4
Mack BaI	1	3	2	5	4
Razumovskii and Chaika BaI	1	4	2	5	3
Jackson and Duong (1963a) BaI	1	4	2	5	3
Kelly and Tomchuk BaII	1	4	2	5	3

6.2 Experimental Considerations

For λ5535 A^{o} the collimation of the beam was 25:1 and the calculated source line width was 1 mK. The collimation of the beam for λ3072 A^{o} was 15:1 giving a source line width of 2 mK. Several collimations between 15:1 and 25:1 were used for λ4934 A^{o} and λ4554 A^{o} with corresponding source line widths of between 1 mK and 2 mK.

The ultraviolet line λ3072A^{o} was examined with aluminum films with a reflection coefficient of 0.85 giving a resolving limit of about $\frac{1}{18}$ of an order (Burridge, Kuhn and Pery[10]). Kodak 103a-0 plates were used for λ3072 A^{o} with exposure times ranging from 1 to 3 hours.

Silver coatings were used for the other three lines. The reflection coefficient for λ5535 A^o was 0.95 giving a resolving limit of about $\frac{1}{60}$ of an order (Kuhn and Wilson[36]). λ5535 A^o was recorded on Kodak 103a-D plates with exposure times between 1/2 and 1-1/2 hours. A few plates were prepared with exposure times up to 7 hours. The silver coatings for λ4934 A^o had a reflection coefficient of 0.90 giving a resolving limit of $\frac{1}{30}$ of an order (Kuhn and Wilson[36]). Kodak 103a-J plates were used for this line and exposure times of between 2 and 4 hours with a few as high as 6 hours. λ4554 A^o was examined with silver coatings having reflection coefficients of 0.85 and 0.90 giving resolving limits of $\frac{1}{18}$ and $\frac{1}{30}$ of an order respectively (Kuhn and Wilson[36]). The line was recorded on 103a-O and 103a-J plates. Exposure times were between 1 and 3 hours.

6.3 BaI Lines λ5535 A^o ($6s^2\ ^1S_o$ - $6s6p\ ^1P_1$) and λ3072 A^o ($6s^2\ ^1S_o$ - $6s7p\ ^1P_1$)

The resonance line of BaI, λ5535 A^o, was studied with a 10 cm etalon. A strong component A and three satellites B, C, D were observed on the high frequency side of A. Plate 4 shows this structure. The positions of the satellites relative to A were measured with a comparator and a microphotometer and were found to be

	A	B	C	D
Separation (in mK)	0	4.4 ± 0.3	10.0 ± 0.3	18.6 ± 0.3
Relative Intensity	14	4.5	4	1

The results quoted are based on comparator measurements of 10 plates and 3 microphotometer tracings. Generally only the results of one order on each plate were used. The errors for the separations are the mean deviations.

The relative intensities of the components were determined from the photometer tracings with an uncertainty of about 20%. The calibration marks were put on the plates with a 7-step density filter. The presence of the strong component A made a large background correction necessary for B and C. This correction was estimated from the shape of the interference fringes and could include a systematic error. Self absorption in the source tends to make the intensities of the components more nearly equal but it should not affect the positions of the components. The long exposures of up to 7 hours indicated no component at +24 mK as suggested by Kopfermann and Wessel. This is in agreement with Jackson (1957). Visual observations of the plates indicated a component found by Jackson (1961) between our components A and B but the resolution was not sufficient to give a numerical value to its position.

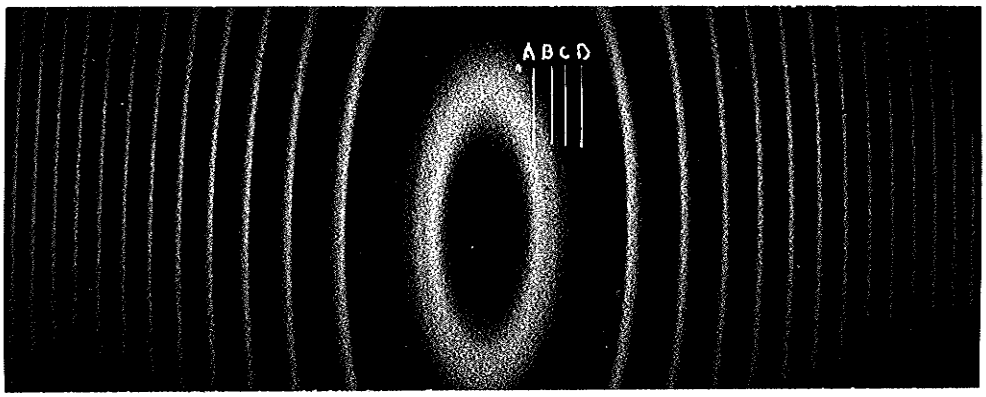

x 17

BaI λ5535 $\mathring{A}$ - 10 cm Spacer

Plate - 4

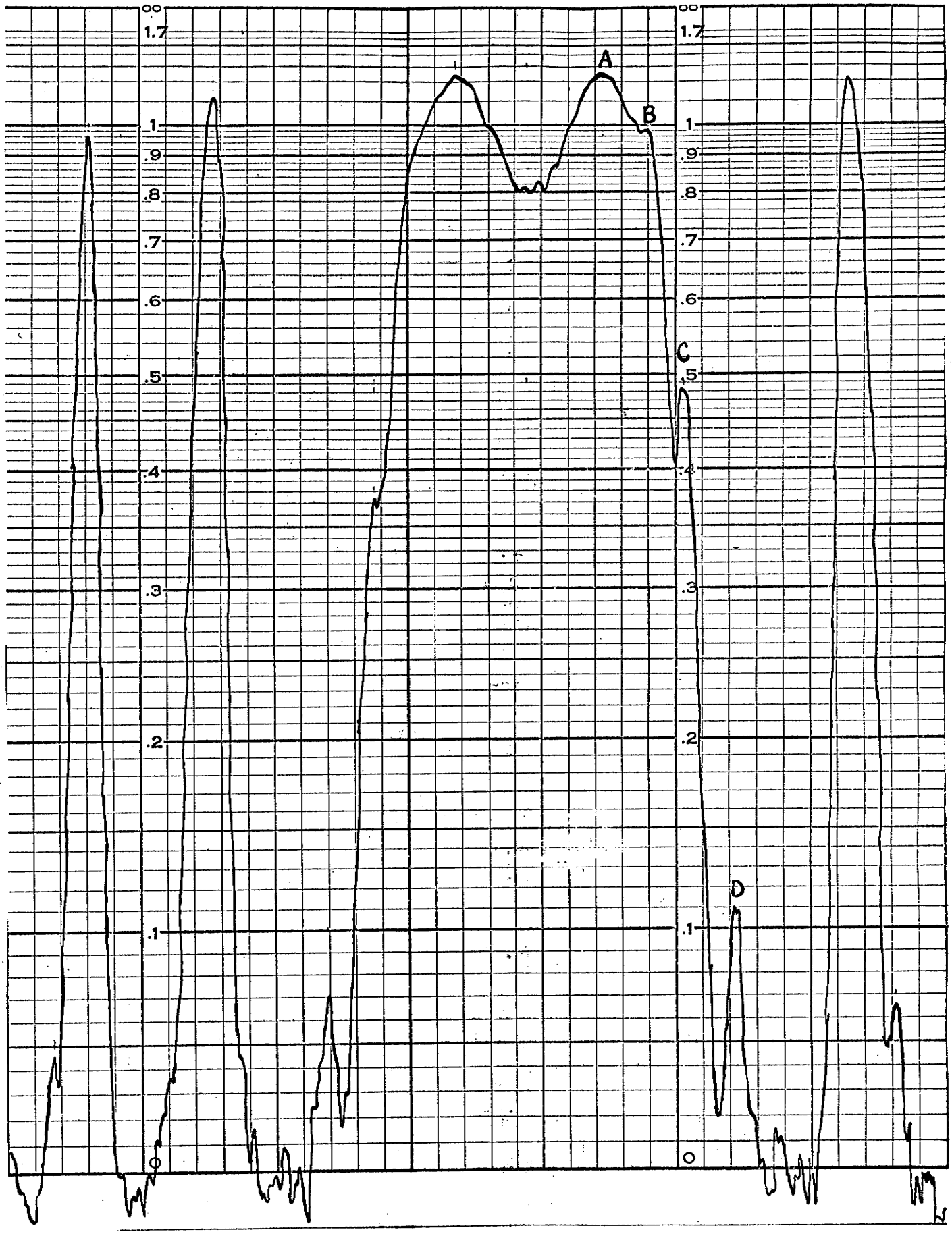

MICROPHOTOMETER TRACING λ 5535 Å

The structure of the second member of the principal singlet series in BaI, λ3072 A^o, was studied with a 10 cm etalon. No clear resolution of structure was observed but a wing on the high frequency side of the fringes 15 mK wide was found.

6.4 BaII Lines λ4934 A^o and λ4554 A^o ($6s\ ^2S_{1/2} - 6p\ ^2P_{1/2,3/2}$)

The structures of the resonance lines of BaII were studied with a variety of etalons.

In λ4934 A^o both the $^2S_{1/2}$ and $^2P_{1/2}$ magnetic hyperfine structures could be resolved so that each odd isotope gives four components with intensity ratios 5:5:1:5. Energy level diagrams are given in Figure 9. Patterns were obtained using 2.534, 4.265 and 10.0 cm etalons (Plates 5). The measurements are summarized below:

No. of orders	Separation (mK) 2.534 cm spacer	Including Pull Correction (mK)
24	$\Delta\gamma(137S_1$, evens) = 123.2 ± 0.7	0
27	$\Delta\gamma(137S_2$, evens) = 71.8 ± 0.7	0
21	$\Delta\gamma(135S_1$, evens) = 105.5 ± 0.8	0
20	$\Delta\gamma(135S_2$, evens) = 59.1 ± 0.6	-.1

continued,

4.265 cm spacer

34	$\Delta\gamma(137S_{3}$, evens) = 37.8 ± 0.6	0
47	$\Delta\gamma(135S_{2}+S_{3}$, evens) = 58.2 ± 0.8	0
31	$\Delta\gamma(137S_{2}$, evens) = 72.5 ± 0.4	0

10.009 cm spacer

16	$\Delta\gamma(138,^{136}_{134})$ = 8.7 ± 0.3	-
11	$\Delta\gamma(138,136)$ = 6.7 ± 0.2	-
16	$\Delta\gamma(138,X)$ = 27.8 ± 0.1	-

The pull of resolved components on each other was estimated from theoretical intensity curves. The errors quoted are the mean deviations. With the 10 cm spacer $\Delta\gamma(138,136)$ was obtained from measurements of the fainter plates while $\Delta\gamma(138,^{136}_{134})$ was obtained from the darker plates. Measurements were to the extreme edge of the wings. The component marked X has a complex structure and is not used in the calculations. Corrections must be made for the influence of unresolved weaker components. Certainly 138 is appreciably influenced by 136 and 134 in the evens. These corrections were estimated by the usual kind of center of gravity calculation. Since these are complicated only the final results will be stated. The calculated values based on the raw data corrected only for the pulls of resolved components will be stated in parentheses.

From these data the magnetic splittings for the $^2S_{1/2}$ level are 238.9 ± 1.5 (237.6 ± 1.5) and 269.1 ± 0.6 (269.1 ± 0.6) mk for 135 and 137 respectively. The ratio of these is 1.126 ± 0.010 (1.133 ± .010) which agrees within experimental error with the more accurate result, 1.119, from magnetic resonance experiments (Hay[19], and Walchi and Rowland[51]). The splittings of the $^2P_{1/2}$ level were found to be 44.8 ± 1.5 (46.4 ± 0.8) and 50.4 ± 0.7 (51.4 ± 0.7) mK for 135 and 137 respectively. The ratio is 1.125 ± 0.056 (1.108 ± 0.034) which also agrees within experimental error with the ratio determined by resonance methods.

Table 10 compares these results for λ4934 A^o with those of Arroe[2]. Our values of the $^2S_{1/2}$ magnetic hyperfine structure are somewhat smaller than those of Arroe and the differences between the two results are a little larger than the combined errors. In each case, however, the ratio of the splittings agrees within experimental error with the more accurate value obtained from magnetic resonance experiments. Our values for the $^2P_{1/2}$ hyperfine structure are about 10% larger than those of Arroe. They are obtained from the measurement of sharp components without reference to the strong 138 component. Arroe's line widths were about 36 mK. This line width is close to the $^2P_{1/2}$ structure and may have influenced the result. Arroe's estimated error for his ratio for the $^2P_{1/2}$ splittings seems too small.

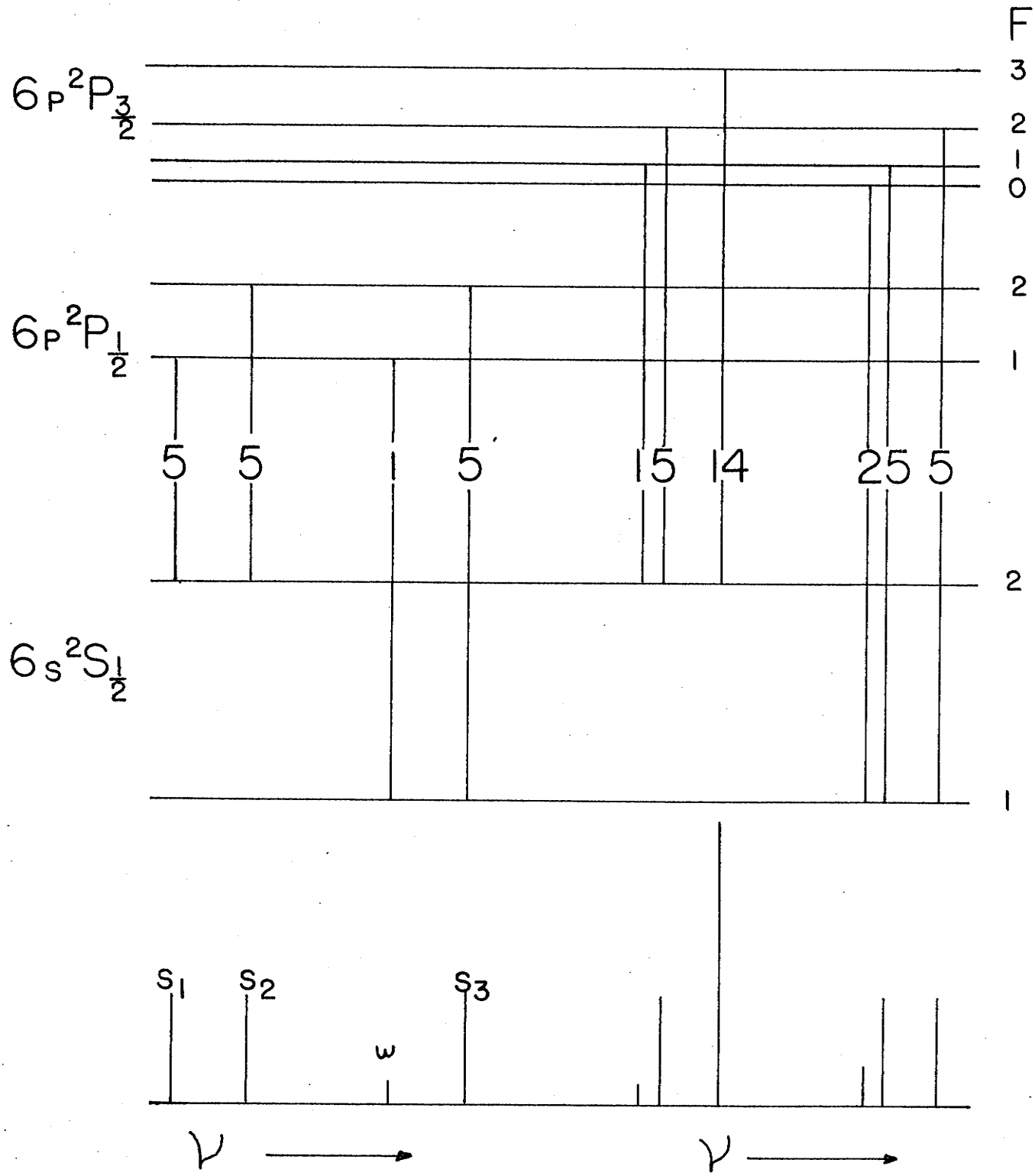

MAGNETIC HFS IN THE B a II LINES

$6s\ ^2S_{\frac{1}{2}} - 6p\ ^2P_{1,2}^{\frac{3}{2}}$

FIGURE – 9

Plates 5

BaII λ4934 A°

2.534 cm spacer

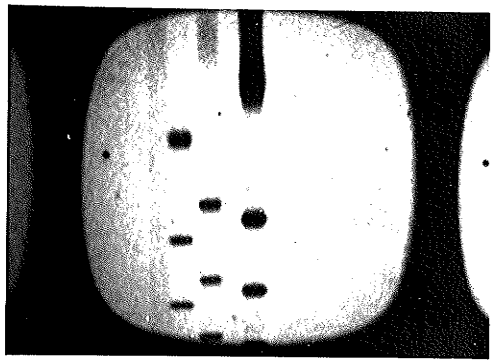

4.265 cm spacer

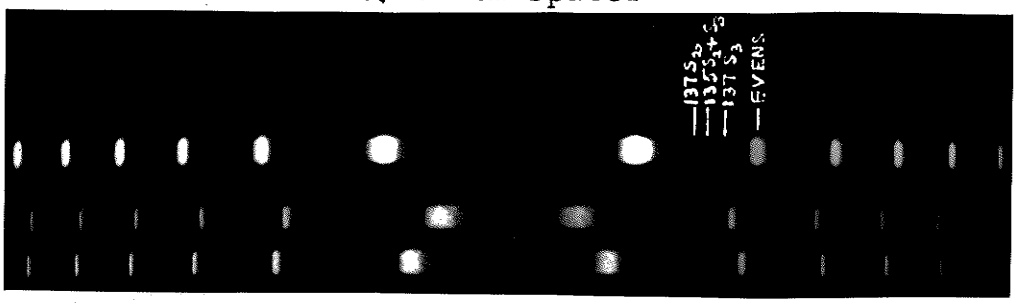

10.009 cm spacer

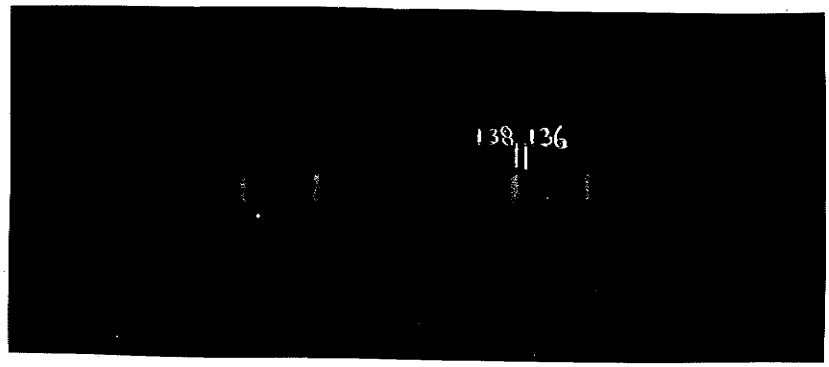

(faint)

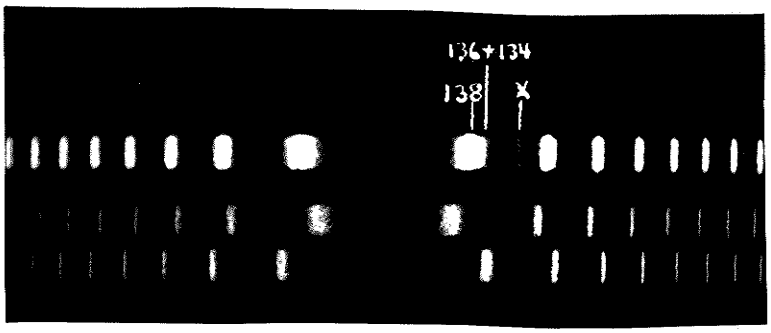

(darker)

Table 10: Magnetic H.F.S. in BaII λ4934 A^{o} (mK)

$^{2}S_{1/2}$

	135	137	Ratio
Arroe	243 ± 1	271 ± 1	1.115 ± .005
Kelly and Tomchuk	238.9 ± 1.5	269.1 ± 0.6	1.126 ± .010

$^{2}P_{1/2}$

Arroe	41.5	46.3	1.113 ± .005
Kelly and Tomchuk	44.8 ± 1.5	50.4 ± 0.7	1.125 ± .056

In λ4554 A^{o} the structure is more complex due to the magnetic hyperfine structure of the $^{2}P_{3/2}$ level. Each odd isotope has six components in two groups separated by the $^{2}S_{1/2}$ structure. The expected structure and component intensities are given in Figure 9.

This line was studied with 1.773, 3.010, 4.999 and 8.009 cm etalons. The patterns obtained appear in Plates 6. The measurements including corrections for the pull of resolved components are summarized below:

No. of orders	Separation (mK)	Including Correction for Pull (mK)
1.773 cm spacer		
28	$\Delta\gamma(W,S) = 40.8 \pm 0.8$	+0.2
30	$\Delta\gamma(S,\text{evens}) = 77.7 \pm 0.7$	0
3.010 cm spacer		
108	$\Delta\gamma(b,\text{evens}) = 80.4 \pm 0.9$	0
28	$\Delta\gamma(a,b) = 16.1 \pm 0.8$	+0.1
28	$\Delta\gamma(b,c) = 13.3 \pm 0.8$	+0.1
4.999 cm spacer		
4	$\Delta\gamma(^{136}_{134},138) = 92.6 \pm 0.8$	-
57	$\Delta\gamma(a,\text{evens}) = 81.9 \pm 0.7$	-0.2
61	$\Delta\gamma(b,\text{evens}) = 68.8 \pm 0.9$	-0.2
54	$\Delta\gamma(c,\text{evens}) = 46.5 \pm 0.8$	-
65	$\Delta\gamma(d,\text{evens}) = 32.0 \pm 0.6$	-
4	$\Delta\gamma(d_1,\text{evens}) = 29.2 \pm 0.5$	-
3	$\Delta\gamma(d_2,\text{evens}) = 37.0 \pm 1.6$	-
8.009 cm spacer		
40 (all readings)	$\Delta\gamma(b,138) = 53.5 \pm 0.9$	-
6 (faintest plates)	$\Delta\gamma(b,138) = 55.2 \pm 0.1$	-
32(darker plates)	$\Delta\gamma(b,138) = 52.8 \pm 0.6$	-
46	$\Delta\gamma(S,138) = 19.1 \pm 0.4$	-
32	$\Delta\gamma(W,138) = 35.9 \pm 0.5$	-
1	$\Delta\gamma(W_1,138) = 39.1$	-
1	$\Delta\gamma(W_2,138) = 31.4$	-

The corrections for pull were estimated from theoretical intensity curves. The errors quoted are the mean deviations. With the 8.009 cm spacer the wing b was measured to the extreme edge. Again these data must be corrected for the influence of unresolved weaker components by center of gravity calculations. Calculated values based on the above raw data are included in parentheses for comparison.

The pattern for the 1.8 cm etalon gives two components for the odd isotopes with a separation of 241.2 ± 0.8 mK. This is an average value for the two odd isotopes and the result agrees with the earlier measurements of Crawford et al[13]. The center of gravity of the odd isotopes is 12.8 ± 0.8 mK on the high frequency side of the center of gravity of the evens. After estimating the influence of 136 and 134 on 138 the center of gravity of the odd isotopes is 13.8 ± 0.8 mK on the high frequency side of 138. This is probably an upper limit as it is possible for the weaker components on the low frequency side not to be blended into the two resolved components.

With the 3 and 5 cm etalons resolution of some of the $^2P_{3/2}$ structure was obtained and the separation of the F = 3 and F = 2 magnetic hyperfine states were found to be 13.3 ± 0.8 (13.3 ± 0.8) and 15.1 ± 0.8 (16.1 ± 0.8) for 135 and 137 respectively. Here the ratio between the two values is 1.135 ± 0.128 (1.211 ± 0.128). The

Plates 6
BaII λ4554 A°

1.773 cm spacer

3.010 cm spacer

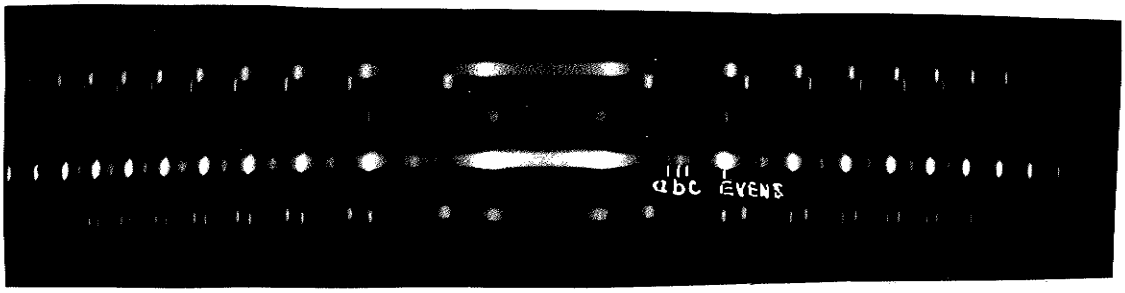

4.999 cm spacer

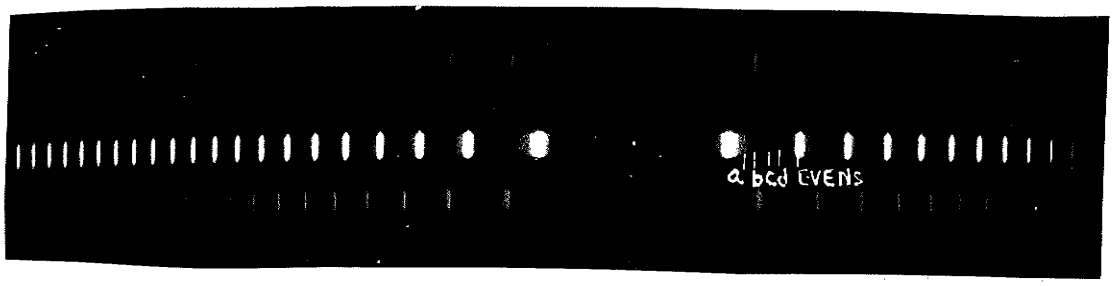

8.009 cm spacer

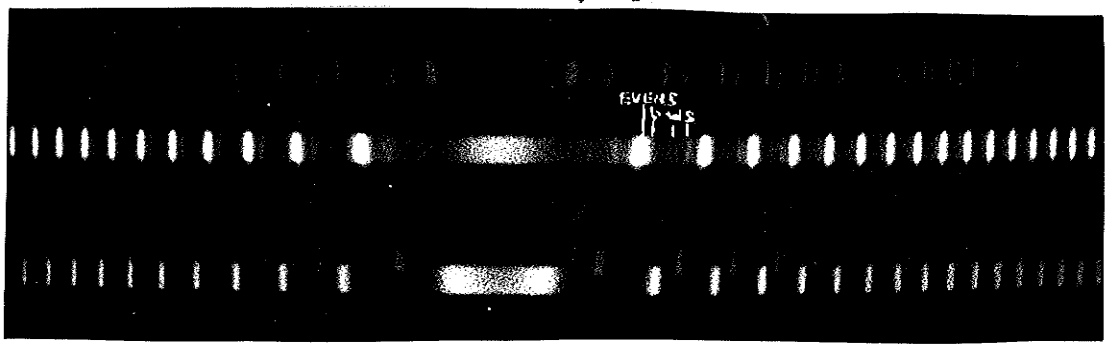

corrected value is in far better agreement with the more accurate value of 1.119. The components were identified by their intensities and the value of the $^2S_{1/2}$ splitting measured in λ4934 A°. No independent value of the $^2S_{1/2}$ splitting was obtained from this line due to the uncertainties introduced by the $^2P_{3/2}$ structure.

The centroids of the odd isotopes relative to 138 can be determined from the observed data. They are found to be +10.1 ± 1.0 (+9.4 ± 1.0) and +13.0 ± 1.5 (+12.2 ± 1.5) for 137 and 135 in λ4934 A°. For λ4554 A° the results of the 3 cm spacer place the centroids of 137 and 135 at 9.8 ± 1.0 (8.4 ± 1.0) and 13.1 ± 1.5 (12.0 ± 1.5) while the results of the 5 cm spacer place them at 8.7 ± 1.0 (6.9 ± 1.0) and 12.0 ± 1.5 (10.6 ± 1.5) mK. The inconsistency between the 3 and 5 cm spacers is believed to be due to the fact that the isotopes 134 and 136 are not as well blended with 138 in the 5 cm spacer as in the 3 cm spacer. Because the even components are not as well blended and because the plates are so overexposed this causes the observer to set the cross hairs of the comparator on the 136 and 134 side of the center of gravity of the evens. This error was estimated from theoretical intensity curves and the measured width of the evens to be about 0.6 mK. The centroids of the odd isotopes calculated from the 5 cm data are then 9.3 ± 1.0 (7.5 ± 1.0) and 12.6 ± 1.5 (11.2 ± 1.5) mK. The results of the 3 cm spacer are considered more

reliable than the results of the 5 cm spacer. The errors are estimated based on the mean deviations in the measurements. These results are summarized in Table 8.

In the patterns with the largest etalons wings on the strong main component were observed in both lines. In the 10 cm spacer for λ4934 A^{o} the wing on the weakly exposed plates extended to +6.7 ± 0.2 mK. This was taken to be the position of 136. On the darker plates the wing extended to +8.7 ± 0.3 mK and this was taken to be the position of 134. In the 8 cm spacer for λ4554 A^{o} the wing on the weakly exposed plates extended to +7.2 ± 0.1 giving the position of 136. The darker plates gave a wing to 9.6 ± 0.6 and this was interpreted as the position of 134. These results appear in Table 8.

The data for λ4934 A^{o} is considered to be more reliable than that for λ4554 A^{o}.

6.5 Discussion of the Results

The results of Jackson and Duong (1963b)[25] show conclusively that the structure observed in λ5535 A^{o} by atomic beam methods is a combination of isotope shift and magnetic hyperfine structure. There is a very satisfactory fit between these (1963b)[25] results and Jackson and Duong's earlier (1963a)[24] isotope shift determinations. Excepting Arroe's[2] position of 136 there is also fair

agreement between all the hollow cathode enriched isotope measurements of λ5535 A^o. The patterns observed in atomic beam measurements (Table 6) can be predicted accurately from Jackson and Duong's (1963b)[25] results.

The structure in λ3072 A^o observed in these experiments gives a qualitative confirmation of this. Since λ3072 A^o involves the same lower level ($6s^2\ ^1S_o$) as λ5535 A^o and the upper level changes only by the excitation of the p electron from 6p to 7p, the field effect shift can be expected to be the same or slightly decreased due to the decreased screening of the 6s electron by the p electron. The isotope shift will be decreased by about 1 mK relative to λ5535 A^o due to changes in the normal mass shift. The formula of Breit and Wills[8] gives a value of $A(6s6p\ ^1P_1) = -4$ mK in agreement with the measured value of -3.6 mKm(Jackson and Duong 1963b)[25]. For $6s7p\ ^1P_1$ a similar calculation gives $A(6s7p\ ^1P_1) = -6$mK with an uncertainty of about 25%. The structure of λ3072 A^o is then expected to be almost entirely due to the magnetic hyperfine structure of the two odd isotopes. The high frequency wing observed on a strong component fits the above estimates.

A major difficulty in the interpretation of the barium isotope shift data is the apparent lack of agreement in the order of the isotopes between Arroe's BaII data and the observations made on λ5535 A^o. In λ5535 A^o both the

odd isotopes are shifted beyond 134 while in BaII 137 lies between 136 and 134.

Our BaII data is not entirely conclusive on the relative positions of the isotopes. The wing on the high frequency side of 138 has been ascribed to 136 and 134 in both λ4554 A^{o} and λ4934 A^{o}. In both lines λ4934 A^{o} and λ4554 A^{o} the most probable position of 137 is beyond 134, although the combined errors of the positions are several times the difference. Due to the difficulties in accurately determining the $^{2}P_{3/2}$ magnetic hyperfine structure and the incomplete resolution of all the components in the pattern the λ4554 A^{o} data is more likely to contain systematic error and hence the λ4934 A^{o} data is the more reliable. The order of the isotopes in both BaII lines is most probably the same as in the λ5535 A^{o}.

There are a number of reasons for a difference in the magnitude of the shifts between BaI and BaII. The normal mass shifts are proportional to frequency and thus are larger in the BaII lines. This difference can, however, be readily calculated and for the isotope pair 137-135 the BaII results should be reduced by 0.2 mK before comparing with BaI. The specific mass effect may have a small contribution but neither the magnitude nor the sense can be estimated with sufficient accuracy from present methods. The expectation, however, is that the effect is small (Kelly and Tomchuk[30] and the present work).

In mercury the shift of a $6s^2$ configuration is 1.6 times that of the 6s configuration (Kopfermann[32]) due to the mutual screening of the two 6s electrons. The shifts in the BaII resonance lines can then be expected to be about 40% larger than in the BaI resonance line.

Our average shift in BaII between 137 and 135 is 3.1 ± 2.5 mK. Arroe's corresponding value is 5.6 ± 1.4. In BaI Jackson and Duong (1963b)[25] observe a shift of 1.1 ± 0.6 mK. If our BaII result is decreased by 40% it becomes 1.9 ± 2.3. The difference between this and the BaI measurement is one quarter the combined errors. Our best value of the shift between 138 and 137 in BaII is 10.1 ± 1.0 mK. Jackson and Duong (1963b)[25] find this shift in BaI to be 7.0 ± 0.3 mK. If the BaII result is decreased by 40% it becomes 6.1 ± 1.0 mK. The difference between this value and the BaI data is within the combined errors of the measurements. Arroe's value of the 138-137 shift is 6.4 ± 0.7 mK. If this is decreased by 40% the difference between Arroe's BaII value and the BaI data is three times the combined error. As pointed out by Razumovskii and Chaika[42], Arroe's result may be influenced by an attempt to keep the spacings of the even isotopes uniform.

The unusual order of the isotopes of barium in the BaI resonance line, where the isotope shift due to removing a single neutron from Ba^{138} to make Ba^{137} is greater than the shift due to the removal of four neutrons to form Ba^{134} is confirmed within the error by observations on the BaII resonance lines.

In Table 11 the isotope shifts obtained for λ4934 A^{o} are compared with the isotope shifts for λ5535 A^{o} obtained by Jackson and Duong. The normal mass effect is subtracted from these shifts. Since indications are that the specific mass effect for an intermediate element is quite small[29,30,47], the residual shifts in row 4 and 8 are due almost entirely to the field or volume effect. The relative isotope shifts in row 5 and 9 show the same trend and give the experimental isotope shift constant C_{exp} on a relative scale. Much of the change in the isotope shift with neutron number N at constant Z is attributed to a nuclear deformation α. The change in the relative isotope shift from isotope pair to isotope pair gives $\frac{\delta C_{exp}}{\delta N} \propto \frac{\delta C_{\alpha}}{\delta N} \propto \frac{\delta^2(\alpha^2)}{\delta N^2}$ on a relative scale. The abrupt change in the relative isotope shift at N = 80 (Z = 56, A = 136) lends support to the idea proposed by Kuhn and Ramsden[37] that the $3s_{1/2}$ neutron shell is the last to be filled.

Table 11: Isotope Shifts in BaI λ5535 A° and BaII λ4934 A° (mK)

λ5535A°

Isotope Pair	138,136	136,134	134,132	132,130	137,135
Measured Shift	+ 4.2	+ 0.4	+ 2.8	+ 0.4	+ 1.1
Normal Mass Effect	- 1.0	- 1.1	- 1.1	- 1.1	- 1.1
Measured Shift minus Normal Mass Effect	+ 5.2	+ 1.5	+ 3.9	+ 1.5	+ 2.2
Relative Shift	1.0	.3	.8	.3	.4

λ4934A°

Measured Shift	+ 6.7	+ 2.0	-	-	+ 2.9
Normal Mass Effect	- 1.2	- 1.2	-	-	- 1.2
Measured Shift minus Normal Mass Effect	+ 7.9	+ 3.2	-	-	+ 4.1
Relative Shift	1.0	.4	-	-	.5

The pronounced staggering in barium means that the odd-neutron nuclei have a smaller effective volume than the even-neutron nuclei. In terms of nuclear deformation this means that the odd-neutron nuclei are less deformed than the even-neutron nuclei. Attempts have been made to explain staggering in terms of nuclear polarization. No complete theory of staggering has been produced as yet.

The experimental isotope shift constant BC_{exp} can be caluclated from equation (1.50) using the isotope shift between 137 and 135 in BaII λ4934 A^{o} which is 2.9 $\pm$ 1.5 mK. The normal mass effect is 1.2 mK. Indications are that the specific mass effect is of the order of the normal mass effect for an intermediate element while the corresponding LiI lines suggest it is in the same sense as the normal mass effect. Hence the total mass effect is 2.4 $\pm$ 1.0 mK. Since the volume and mass effects are in the opposite sense, $\beta^{*}\delta\Delta T_{s}$ is 5.3 $\pm$ 2.5 mK. Using n_{o} = 2.332, Z_{o} = 2 and $1 - \frac{d\sigma}{dn}$ = 1.092 in equation (1.50) it is found that βC_{exp} (Ba 135,137) = 15 $\pm$ 7 mK. The other isotope shift constants are related to the above as the relative isotope shifts.

CONCLUSION

Before isotope shifts can be used to obtain information about such nuclear properties as size and shape one must determine the contribution made to the isotope shift by the specific mass effect. The present study of various spectral lines of cadmium indicates that the contribution made to the isotope shift in elements above cadmium in the periodic table is small, although an appreciable effect could result from an unusual electronic configuration. In particular the cadmium study led to the determination of the specific mass integral K(5s,5p). The comparison of this integral with others of the form K(ns,np) where $n < 5$ indicated that these integrals were likely to decrease in value beginning with $n = 5$. The work on barium confirmed that the odd isotopes of barium exhibit an unusually pronounced odd-even staggering. It also showed that the ordering of the isotopes in the BaII resonance lines is the same as in the BaI singlet resonance line. This is in disagreement with the results reported by Arroe for BaII. The agreement between the relative isotope shifts in the singlet resonance line and the BaII line λ4934 A^{o} is further evidence that the specific mass effect in the intermediate elements is small. The isotope shift indicates that the effective volumes of the isotopes 137 and 135 are smaller than the effective volume of 134 and that the change in effective volume from 138 to 136 is much greater than the change in the effective volume from 136 to 134.

REFERENCES

1. Araki, G., Mano, K., and Ohta, M., Phys. Rev., 115, 1222, 1959.

2. Arroe, A. H., Phys. Rev., 79, 836, 1950.

3. Bacher, R. F., and Goudsmit, S., Atomic Energy States, McGraw-Hill Book Company, New York, 1932.

4. Bainbridge, K. T., and Nier, A. O., Nuclear Science Series, Preliminary Report, No. 9, N.R.C., U.S.A., 1950.

5. Bartlett, J. H., and Gibbons, J. J., Phys. Rev., 44, 538, 1933.

6. Bradley, L. C., and Kuhn, H. G., Proc. Roy. Soc. A, 209, 325, 1951.

7. Breit, G., Theory of Isotope Shift, Reviews of Modern Physics, Vol. 30, No. 2, 507, 1958.

8. Breit, G., and Wills, L., Phys. Rev., 44, 470, 1933.

9. Brix, P., and Kopfermann, H., Isotope Shift Studies of Nuclei, Reviews of Modern Physics, Vol. 30, No. 2, 517, 1958.

10. Burridge, J. C., Kuhn, H., and Pery, A., Proc. Phys. Soc., B.66, 963, 1953.

11. Crawford, M. F., et al, Canadian Journal of Physics, A.28, 558, 1950.

12. Crawford, M. F., et al, Canadian Journal of Physics, A.28, 138, 1950.

13. Crawford, M. F., Kelly, F. M., and Kurz, W., Unpublished data, University of Toronto, 1950.

14. Condon, E. U., Shortley, G. H., The Theory of Atomic Spectra, Cambridge University Press, 1953.

15. Fred, M., and Tomkins, F. S., et al, Phys Rev., 82, 406, 1951.

16. Gray, W. M., Ph.D. Thesis, University of Toronto, 1949.

17. Green, J. B., and Loring, R. A., Rev. Sci. Inst., 11, 41, 1940.

18. Hately, G. F., and Littlefield, T. A., J. Opt. Soc. Amer., 48, 851, 1958.

19. Hay, R. H., Phys. Rev., 60, 75, 1941.

20. Hughes, D. S., and Eckart, C., Phys. Rev., 36, 694, 1930.

21. Hughes, R. H., Phys. Rev., 105, 1260, 1957.

22. Jackson, D. A., Phys. Rev., 106, 948, 1957.

23. Jackson, D. A., Proc. Roy. Soc. A 263, 289, 1961.

24. Jackson, D. A., and Duong, H. T., Proc. Roy. Soc., A274, 145, 1963.

25. Jackson, D. A., and Duong, H. T., Phys. Rev. Letters, 11, 209, 1963.

26. Kelly, F. M., Ph.D. Thesis, University of Toronto, 1949.

27. Kelly, F. M., Can. J. Phys., 35, 1220, 1957.

28. Kelly, F. M., Determination of Nuclear Spins and Magnetic Moments by Spectroscopic Methods, Handbuch der Physik, 38, 59, 1958.

29. Kelly, F. M., and Tomchuk, E., Proc. Phys. Soc. A, 74, 689, 1959.

30. Kelly, F. M., and Tomchuk, E., Proc. Phys. Soc. 78, 1304, 1961.

31. Kelly, F. M., and Tomchuk, E., Canad. J. Phys., 42, 918, 1964.

32. Kopfermann, H., Nuclear Moments, Academic Press, New York, 1958.

33. Kopfermann, H. and Wessel, G., Nachr. Akad. Wiss. Göttingen, Math-physik, Kl. No. 2, 53, 1948.

34. Kopfermann, H. and Wessel, G., Nachr. Akad. Wiss. Göttingen, Math-physik, Kl. No. 3, 1, 1951.

35. Kuhn, H. G., Atomic Spectra, Longmans, 1962.

36. Kuhn, H., and Wilson, B. A., Proc. Phys. Soc. B63, 745, 1950.

37. Kuhn, H. G. and Ramsden, S. A., Proceedings of the Royal Society, A., 237, 485, 1956.

38. Kuhn, H., New Techniques In Optical Interferometry, Reports On The Progress In Physics XIV, 64, 1951.

39. Mack, J. E., Phys. Rev. 109, 820, 1958.

40. Meissner, K. W., Rev. Mod. Phys., 14, 68, 1942.

41. Pauli, W., and Peierls, R. E., Phys. Z., 32, 670, 1931.

42. Razumovskii, A. N., and Chaika, M. P., Opt. i Spektr. 12, 338, 1962; Optics and Spectroscopy 12, 186, 1962.

43. Schawlow, A. L., Ph.D. Thesis, University of Toronto, 1949.

44. Slater, J.C, Phys. Rev., 34, 1293, 1929.

45. Stone, A. P., Proc. Phys. Soc. A68, 1152, 1955.

46. Sutherland, J. B., M.Sc. Thesis, University of Manitoba, 1957.

47. Tomchuk, E., M.Sc. Thesis, University of Manitoba, 1959.

48. Tolansky, S., High Resolution Spectroscopy, Methuen and Co., Ltd., London, 1947.

49. Vinti, J. P., Phys. Rev., 56, 1120, 1939.

50. Vinti, J. P., Phys. Rev. 58, 882, 1940.

51. Walchi, H. E., and Rowland, T. J., Phys. Rev. 102, 1334, 1956.

52. Wilets, L., Isotope Shifts, Handbuch der Physik, 38, 96, 1958.

53. Williams, W. Ewart, Applications of Interferometry, Methuen and Co., Ltd., London, 2nd ed., 1941.

ACKNOWLEDGEMENTS

This research project was under the stimulating direction of Dr. F. M. Kelly, Professor in the Department of Physics and was supported by a grant from the National Research Council of Canada.

The author is indebted to Dr. A. E. Douglas of the National Research Laboratory, Ottawa, for preparing the microphotometer traces of the BaI line 5535 A^{o}.

The author would like to thank Mr. T. Saunders for preparing the photographs, Mr. R. Parr for preparing the ozlids, and Miss B. Hartland for typing the thesis.

APPENDIX A

REPRINTED FROM THE
PROCEEDINGS OF THE PHYSICAL SOCIETY, VOL. LXXIV, p. 689, 1959

PRINTED IN GREAT BRITAIN

Isotope Shift in the CdI Intercombination Resonance Line λ 3261 Å

BY F. M. KELLY AND E. TOMCHUK
Department of Physics, University of Manitoba, Winnipeg, Canada

MS. received 2nd June 1959, in final form 3rd July 1959

Abstract. The isotope shifts in the intercombination resonance line of CdI have been measured. The line was excited in an atomic beam by electron bombardment and the high resolution obtained with a Fabry–Perot interferometer. The shifts between even isotopes decrease with increasing neutron number and the odd isotopes lie close to the next lighter even isotope showing a pronounced odd–even staggering. The relative shifts are in agreement with those of other Cd lines.

§ 1. INTRODUCTION

CADMIUM has six stable even isotopes and two stable odd isotopes so that it is ideal for isotope shift studies. The relative abundances of the naturally occurring isotopes (Bainbridge and Nier 1950) are given in table 1.

Table 1

Isotope	106	108	110	111	112	113	114	116
Abundance (%)	1·22	0·88	12·4	12·8	24·1	12·3	28·8	7·6

Isotope shifts in the intercombination resonance line λ3261 ($5s^2\ ^1S_0 - 5s5p\ ^3P_1$) were first measured by Brix and Steudel (1950) who used the absorption of six atomic beams in series. They measured the relative separations of isotopes 110, 112 and 114.

In this experiment an atomic beam was excited by electron bombardment and λ3261 was observed in emission. The isotope shifts between 106, 110, 111, 112, 113, 114 and 116 were observed.

Isotope shifts for cadmium have also been measured by several authors in the spark line λ4416 ($4d^{10}\,5p\ ^2P_{3/2} - 4d^9\,5s^2\ ^2D_{5/2}$). The most recent measurements are those of Kuhn and Ramsden (1956) who used enriched isotopic samples and a hollow cathode cooled with liquid hydrogen. They measured the shifts between all of the stable isotopes.

In the heavy elements the isotope shifts can be explained by the field or volume effect. For the light elements isotope shifts arise from the two mass effects. The normal mass effect can be accounted for by a reduced mass calculation. The specific mass effect which arises from the interaction between the electrons is difficult to calculate. Both mass effects decrease with increasing mass number but it is not certain where the specific effect becomes negligible. The shifts reported here were measured to redetermine the ratios of Kuhn and Ramsden using a different line to check the possible influence of a residual specific mass effect.

The spins of both the odd isotopes are known to be $\frac{1}{2}$ and the nuclear magnetic moments are negative (Strominger, Hollander and Seaborg 1958). Then

each odd isotope gives rise to two components in λ3261 Å. The weaker component has the higher wave number.

§ 2. Experimental Arrangement

An atomic beam light source essentially similar to that described by Crawford *et al.* (1950) was constructed. The beam of cadmium atoms was produced by evaporating cadmium from a wire wound iron furnace heated by an electrical current. The collimation of the beam was 14, so that the source line width was $0{\cdot}002\,\mathrm{cm}^{-1}$.

The beam was excited by electron bombardment with low speed electrons. The line λ3261 was isolated with a Hilger medium quartz spectrograph and the high resolution was supplied by a quartz Fabry–Perot interferometer mounted externally to the spectrograph. Spacers of 3 and 5 cm were used.

The interferometer plates were coated with aluminium films each of which had a transmission coefficient of about 0·03 in the visible region. This corresponds to a reflection coefficient of about 0·85 at a wavelength of 3200 Å (Burridge, Kuhn and Pery 1953). Eastman 103aO plates were used. The exposure times varied between ten minutes and one hour.

§ 3. Results

The 5 cm etalon gave good resolution for the four most abundant even isotopes. The four components to be expected for the odd isotopes were thrown in the inter-order space and three components were observed. One of these three was due to a superposition of two components. The components are named according to the mass number of the isotope of origin. The two components from each of the odd isotopes are designated as s or w to indicate the strong and weak components.

With the 5 cm spacer the components 113w and 111s were not resolved. With a 3 cm spacer the components 111s and 113s were well separated and could be easily measured. However the resolution was not as high, and, there was interference between the two weak components of the odd isotopes and the even components, so that measurements of the even components from these plates were not used in the calculations. The results of the measurements are summarized in table 2.

Table 2

Isotope pair	No. of fringes measured	Etalon spacer (cm)	Separation ($\times 10^{-3}$ cm^{-1})
114, 116	81	5	$9{\cdot}3 \pm 0{\cdot}3$
112, 114	301	5	$13{\cdot}5 \pm 0{\cdot}4$
110, 112	98	5	$16{\cdot}3 \pm 0{\cdot}5$
112, 113s	88	5	$26{\cdot}1 \pm 0{\cdot}4$
112, 111w	69	5	$51{\cdot}5 \pm 0{\cdot}4$
112, 113w+111s	69	5	$44{\cdot}0 \pm 0{\cdot}4$
112, 106	24	3	$51{\cdot}7 \pm 1{\cdot}7$
113s, 111s	164	3	$19{\cdot}8 \pm 0{\cdot}3$

Theoretical intensity curves were plotted to estimate the displacement of the peak of 116 due to the presence of the much stronger component due to 114. The correction was estimated to be $0{\cdot}0002\,\mathrm{cm}^{-1}$ and has been included in table 2. Similar corrections were applied to other components which were close together

in the observed patterns. The errors quoted in table 2 are probable errors obtained by multiplying the average deviations from the means by 0·68. Some twenty exposures with each spacer were measured five times by each of two observers with a comparator. The number of fringes measured is given in table 2.

The shifts between the various even isotopes are given directly by table 2. However, the centres of gravity of the components due to the odd isotopes must be calculated before the relative isotope shifts can be estimated.

From table 2, $\Delta\nu(112, 111w) = 151{\cdot}5$. 111w is overlapped one order in the pattern. Also from table 2, $\Delta\nu(112, 113s) = 100{\cdot}0 - 26{\cdot}1 = 73{\cdot}9$. From the 3 cm etalon measurements $\Delta\nu(113s, 111s) = 19{\cdot}8$ so that $\Delta\nu(112, 111s) = 54{\cdot}1$. The total magnetic hyperfine structure splitting for 111 is the sum of $\Delta\nu(112, 111w)$ and $\Delta\nu(112, 111s)$ and is 205·6.

For isotope 113, $\Delta\nu(112, 113s)$ is measured directly from the 5 cm patterns and is 73·9. The direct measurements also give $\Delta\nu(112, 113w + 111s) = 44{\cdot}0$. From the information concerning isotope 111, 111s lies 1·9 to the higher frequency side of the measured centre of gravity of 113w and 111s in the 5 cm patterns. Then, weighting 111s and 113w according to known relative abundances and statistical weights, 113w lies 3·9 to the low-frequency side of the centre of gravity of 113w and 111s. Thus, in the 5 cm pattern 113w is 40·1 to the high-frequency side of 112 and $\Delta\nu(112, 113w) = 140{\cdot}1$. Then, the magnetic hyperfine structure for 113 is $73{\cdot}9 + 140{\cdot}1 = 214{\cdot}0$. The unit in these separations is $10^{-3}\,\mathrm{cm}^{-1}$.

A check on the accuracy of these results can be made by a comparison with the ratio of the nuclear magnetic moments from other determinations. From our measurements

$$\frac{\mu 113}{\mu 111} = \frac{214{\cdot}0}{205{\cdot}6} = 1{\cdot}041.$$

This agrees well with the nuclear induction measurements of Proctor and Yu (1950) which give a ratio of 1·046 for these two nuclear moments.

From the above measurements the centres of gravity of the odd isotopes can be placed relative to the even ones and we find

$$\Delta\nu(112, 113) = 2{\cdot}4 \pm 1{\cdot}3 \times 10^{-3}\,\mathrm{cm}^{-1}$$
$$\Delta\nu(110, 111) = 1{\cdot}8 \pm 1{\cdot}6 \times 10^{-3}\,\mathrm{cm}^{-1}$$

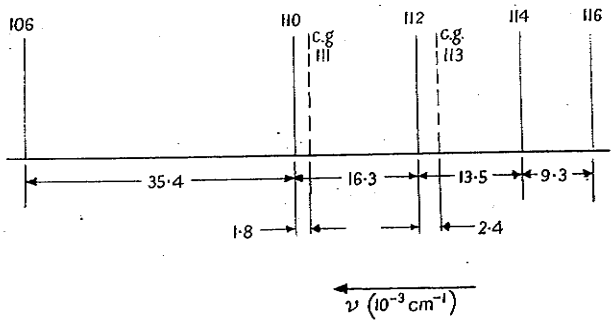

Isotope shifts in CdI λ 3261.

The order of the isotopes is regular. A summary of our observed shifts is given in the figure.

§ 4. Isotope Shift

The observed isotope shifts in λ3261 need to be adjusted for the normal mass shift. Table 3 gives the values of the shifts when the normal mass effect has been taken into account.

Table 3

Isotope pair	114, 116	112, 114	110, 112	106, 110	111, 113
Isotope shift $\times(10^{-3}\ \mathrm{cm}^{-1})$	$11{\cdot}8\pm0{\cdot}4$	$16{\cdot}1\pm0{\cdot}4$	$19{\cdot}0\pm0{\cdot}5$	$40{\cdot}8\pm2{\cdot}1$	$19{\cdot}5\pm2{\cdot}4$

Following Kuhn and Ramsden the relative shifts between the various isotopes are calculated using $\Delta\nu(110, 112)=1{\cdot}00$. In table 4 the results are compared.

Table 4

Isotopes	Relative shift	
	This paper	Kuhn and Ramsden
$(106, 110)\frac{1}{2}$	1·07	1·04
108, 110	–	1·00
110, 112	1·00	1·00
111, 113	1·03	1·03
112, 114	0·85	0·93
114, 116	0·62	0·65

These ratios agree within experimental error with those of Kuhn and Ramsden (1956) except for the ratio (112, 114). In this case the observed difference is 9% whereas the sum of the experimental errors is 7%. However we have made visual measurement only so that there may be a small and unknown systematic error in our results. To this extent the results of Kuhn and Ramsden are confirmed.

§ 5. Magnetic Moment

The measurement of the magnetic hyperfine structure of the odd isotopes enables a calculation of the nuclear magnetic moments. From the formula for intermediate coupling (Breit and Wills 1933) we obtain $\mu(113)=-0{\cdot}55$ n.m. and $\mu(111)=-0{\cdot}52$ n.m. These values are about 12% lower than the results from nuclear induction (Proctor and Yu 1950).

The spectroscopic values calculated in this way may be expected to be low for we have used the value of a_{5s} determined from data for Cd II whereas in fact the 5s electron is screened by the 5p electron. A reduction of a_{5s} by 10% to allow for the screening to the 5p will bring the two values into agreement.

Acknowledgments

The research reported here was supported by a grant from the National Research Council of Canada. One of us (E.T.) is indebted to the Northern Electric Company of Canada for a research scholarship.

References

Bainbridge, K. T., and Nier, A. O., 1950, *Nuclear Science Series, Preliminary Report* No. 9 N.R.C. U.S.A.

Breit, G., and Wills, L. A., 1933, *Phys. Rev.*, **44**, 470.

Brix, P., and Steudel, A., 1950, *Z. Phys.*, **128**, 260.

Burridge, J. C., Kuhn, H., and Pery, A., 1953, *Proc. Phys. Soc.* B, **66**, 963.

Crawford, M. F., Schawlow, A. L., Kelly, F. M., and Gray, W. M., 1950, *Canad. J. Phys.*, A, **28**, 558.

Kuhn, H. G., and Ramsden, S. A., 1956, *Proc. Roy. Soc.* A, **237**, 485.

Proctor, W. G., and Yu, F. C., 1950, *Phys. Rev.*, **76**, 1728.

Strominger, D., Hollander, J. M., and Seaborg, G. T., 1958, *Rev. Mod. Phys.*, **30**, 585.

APPENDIX B

REPRINTED FROM THE
PROCEEDINGS OF THE PHYSICAL SOCIETY, VOL. LXXVIII, p. 1304, 1961

PRINTED IN GREAT BRITAIN

Isotope Shift in the CdI Resonance Line λ 2288 Å

By F. M. KELLY and E. TOMCHUK
Department of Physics, University of Manitoba, Winnipeg, Canada

MS. received 19th June 1961

Abstract. The isotope shifts in the singlet resonance line of CdI have been observed. The line was excited by electron bombardment of an atomic beam and the high resolution was obtained with a Fabry–Pérot interferometer. The shifts measured in this line (λ 2288 Å) are compared with those previously measured in the intercombination resonance line (λ 3261) to show that the specific mass effect is small. Comparisons are made with similar measurements in magnesium, zinc, and strontium.

§ 1. Introduction

There are two causes of isotope shift in atomic spectra, the mass effect and the field or volume effect. In the light elements the observed shifts can be accounted for by the mass effect while in the heaviest elements the shifts are attributed to the field effect. The mass effect can conveniently be separated into the normal mass effect and the specific mass effect (Hughes and Eckart 1930, Bartlett and Gibbons 1933, Vinti 1939, 1940). The normal mass effect is easily determined from a simple reduced mass calculation and thus can be taken into account in all atomic energy levels. The specific mass effect, on the other hand, requires the computation of a number of integrals involving the products of radial wave functions of the atomic levels, and, except in the case of helium, has achieved only moderate success. Both mass effects decrease with increasing atomic number but it is not certain where the specific mass effect can be neglected. It is possible, however, to make an experimental estimate of the specific effect by comparing the shifts in a pair of lines. Such a pair is the singlet and intercombination resonance lines of cadmium.

The singlet resonance line λ 2288($5s^2\ {}^1S_0$–$5s5p\ {}^1P_1$) and the intercombination resonance line λ 3261($5s^2\ {}^1S_0$–$5s5p\ {}^3P_1$) have a common lower level. The upper levels arise from the same (5s5p) electronic configuration. The field effect shift of either a $p_{1/2}$ or a $p_{3/2}$ electron is small compared to the shift due to an s electron so that the shift arising from the field effect should be the same in both these lines. The specific mass effect, however, predicts that the shifts of these two lines should differ by an amount depending only on K(5s, 5p), one of the specific mass integrals in the notation of Bartlett and Gibbons (1933).

Isotope shifts in λ 3261 have already been reported (Kelly and Tomchuk 1959). The shifts observed in λ 2288 are reported here, and are compared with the shifts in λ 3261. Similar comparisons in lighter elements have been made for zinc (Crawford *et al.* 1950), magnesium (Kelly 1957) and strontium (Hughes 1957).

§ 2. Experimental Arrangements

The singlet resonance line was excited in the atomic beam source used for the study of λ3261. The collimation of the beam was such that the calculated source line width was 0·002 cm^{-1}. The line was isolated with a Hilger medium quartz spectrograph and the high resolution was supplied with a quartz Fabry–Pérot interferometer mounted externally to the spectrograph. A 10 cm spacer was used. The reflectivity of the aluminium films at λ2288 Å was estimated to be 80% from the measured transmission coefficient in the blue and the curves of Burridge, Kuhn and Pery (1953). The patterns were recorded on Ilford QI and QII plates with exposure times up to two hours.

§ 3. Results

The line λ2288 was resolved into three closely spaced components. Twenty-five exposures with structure in two to five orders were measured five times by each of two observers. Microphotometer measurements were not satisfactory due to the curvature of the fringes. The three components are designated A, B and C with A having the highest frequency. The measured separations are

$$\Delta\nu(\mathrm{A,\ B}) = 16{\cdot}8 \pm 0{\cdot}3 \times 10^{-3}\ \mathrm{cm}^{-1}$$
$$\Delta\nu(\mathrm{B,\ C}) = 12{\cdot}5 \pm 0{\cdot}5 \times 10^{-3}\ \mathrm{cm}^{-1}.$$

The errors quoted are the average deviations from the mean multiplied by 0·68.

The assignment of component A to a blend of components due to isotopes 110 and 111, component B to a blend of components due to isotopes 112 and 113 and C to isotope 114 is consistent with visually estimated relative intensities.

The unresolved separations of the isotope pairs (110–111) and (112–113) were assumed to be in the ratio found in λ3261, and, by Kuhn and Ramsden (1956), in λ4416. Then, if we use the relative abundance as a weight factor the separations between even isotopes can be calculated. These calculations give

$$\Delta\nu(110\text{–}112) = -17{\cdot}0 \pm 0{\cdot}6 \times 10^{-3}\ \mathrm{cm}^{-1}$$
$$\Delta\nu(112\text{–}114) = -13{\cdot}2 \pm 1{\cdot}0 \times 10^{-3}\ \mathrm{cm}^{-1}.$$

In this the error has been doubled to allow for the extra uncertainties introduced. We also assumed that the magnetic hyperfine structure in the $^1P_1$ level is negligible. The negative sign means the lighter isotope has the higher frequency.

A plot of theoretical curves shows that the influence of isotope 116 on the position of isotope 114 is much less than the experimental error.

§ 4. Discussion

The isotope shifts between even isotopes in the singlet (λ2288) and the intercombination (λ3261) resonance lines may be analysed in a manner similar to that used for the Zn I resonance lines (Crawford *et al.* 1950).

Table 1. Isotope Shift in Cd I (in $10^{-3}\ cm^{-1}$)

	2288		3261	
	110–112	112–114	110–112	112–114
Observed shift	−17·0	−13·2	−16·3	−13·5
Normal shift	+ 3·4	+ 3·7	+ 2·7	+ 2·6
Residual shift ($\Delta\nu$)	−20·9	−16·9	−19·0	−16·1
3261–2288 ($\delta(\Delta\nu)$)	+ 1·9	+ 0·8		

The residual shift ($\Delta\nu$) is the observed shift minus the normal mass shift. The differences between the residual shifts are $+1{\cdot}9 \pm 1{\cdot}1$ for (110–112) and $+0{\cdot}8 \pm 1{\cdot}4$ for (112–114). These two values agree within experimental error and the average is $+1{\cdot}3 \pm 1{\cdot}3$.

The difference between the isotope shifts in the triplet and the singlet resonance lines according to the specific mass theory (Bartlett and Gibbons 1933) is

$$\delta(\Delta\nu)\ (\text{triplet–singlet}) = -4Rm\left\{\frac{1}{M_1} - \frac{1}{M_2}\right\} K(n\text{s}, n\text{p})$$

where R is the Rydberg constant (cm^{-1}), m the electron mass, M_1, M_2 the nuclear masses ($M_2 > M_1$), and K the specific mass integral which is intrinsically negative. The data for Mg (Kelly 1957), Zn (Crawford *et al.* 1950, Hately and Littlefield 1958), Sr (Hughes 1957) and Cd for the shifts arising from isotopes differing by two neutrons are summarized in Table 2.

Table 2

	n	$\delta(\Delta\nu)$ Triplet–singlet ($\times 10^{-3}\ \text{cm}^{-1}$)	$K(n\text{s}, n\text{p})$
Mg	3	$+57{\cdot}9 \pm 1{\cdot}6$	$-0{\cdot}076 \pm 0{\cdot}002$
Zn	4	$+10 \pm 1{\cdot}5$	$-0{\cdot}091 \pm 0{\cdot}014$
Sr	5	$+5{\cdot}6 \pm 1{\cdot}8$	$-0{\cdot}033 \pm 0{\cdot}024$
Cd	5	$+1{\cdot}3 \pm 1{\cdot}3$	$-0{\cdot}03 \pm 0{\cdot}03$

The value of the specific mass integral $K(n\text{s}, n\text{p})$ is not very sensitive to the value of the principal quantum number n, and for $n = 5$ appears to be decreasing. The factor $\Delta M/M_1M_2$ in the heavy elements will reduce the resulting specific mass shifts to small values. Consequently in the heavy elements one can expect to obtain specifically nuclear data from the observed isotope shifts.

Acknowledgments

The research reported here was supported by a grant from the National Research Council of Canada.

References

Bartlett, J. H., and Gibbons, J. J., 1933, *Phys. Rev.*, **44**, 538.
Burridge, J. C., Kuhn, H. G., and Pery, A., 1953, *Proc. Phys. Soc.* B, **66**, 963.
Crawford, M. F., Gray, W. M., Kelly, F. M., and Schawlow, A. L., 1950, *Canad. J. Res.* A, **28**, 138.
Hately, G. F., and Littlefield, T. A., 1958, *J. Opt. Soc. Amer.*, **48**, 851.
Hughes, D. S., and Eckart, C., 1930, *Phys. Rev.*, **36**, 694.
Hughes, R. H., 1957, *Phys. Rev.*, **105**, 1260.
Kelly, F. M., 1957, *Canad. J. Phys.*, **35**, 1220.
Kelly, F. M., and Tomchuk, E., 1959, *Proc. Phys. Soc.* A, **74**, 689.
Kuhn, H. G., and Ramsden, S. A., 1956, *Proc. Roy. Soc.* A, **237**, 485.
Vinti, J. P., 1939, *Phys. Rev.*, **56**, 1120.
—— 1940, *Phys. Rev.*, **58**, 882.

APPENDIX C

ISOTOPE SHIFT IN BARIUM

F. M. KELLY AND E. TOMCHUK

ISOTOPE SHIFT IN BARIUM

F. M. KELLY* AND E. TOMCHUK
Department of Physics, University of Manitoba, Winnipeg
Received December 2, 1963

ABSTRACT

Isotope shifts and magnetic hyperfine structures for lines in the first and second spectra of barium are reported and compared with previous results in an attempt to remove anomalies which have existed in isotope-shift determinations. The unusual order of the barium isotopes in the Ba I resonance line has been partially confirmed by observations on Ba II.

INTRODUCTION

Barium has seven stable isotopes, the abundances of which are listed in Table I. The proximity of the magic neutron number 82 makes isotope-shift measurements of interest.

TABLE I

Isotope	138	137	136	135	134	132	130
Abundance (%)	71.7	11.3	7.8	6.6	2.4	0.096	0.103

There have been a number of experiments to determine isotope shifts in the resonance line of Ba I. Kopfermann and Wessel (1948, 1951) first used an atomic beam to absorb the resonance line λ 5535 ($6s^2\ ^1S_0$–$6s6p\ ^1P_1$) and later used an atomic beam excited by resonance fluorescence. They observed no clear resolution of components and interpreted the wing on the high-frequency side of the main component as being the result of isotope shift alone. Their weak component at +24 mK (1 mK = 10^{-3} cm^{-1}) is supported by absorption data only and may be neglected. The results are summarized in Table II.

TABLE II

Atomic beam observations (mK)* λ5535 ($6s^2\ ^1S_0$–$6s6p\ ^1P_1$)

Kopferman and Wessel (1948)	0	—	+7	+12	+18	+24
Crawford *et al.*	0	—	—	+ 9.7	+17.2	—
Jackson (1957)	0	—	+3.8	+ 9.9	+18.4	—
Jackson (1961)	0	+2.0	+3.9	+ 9.1	+18.1	—
Kelly and Tomchuk	0	—	+4.4	+10.0	+18.7	—

*The strongest component is taken as zero.

In a later investigation Arroe (1950) employed hollow-cathode sources cooled with liquid air and containing various samples of enriched isotopes. The wavelengths of the light emitted by the various samples were compared

*Present address: Department of Physics, University of Otago, Dunedin, New Zealand.

with a Fabry–Pérot interferometer. The magnitudes of the isotope shifts in λ 5535 derived by Arroe are given in Table III. They differ markedly from the data of Kopfermann and Wessel.

TABLE III

Isotope shift in Ba I (mK) λ5535 ($6s^2\ ^1S_0$–$6s6p\ ^1P_1$)

	Isotope:						
	138	137	136	135	134	132	130
Arroe	0	+5.2	+2.2	+ 7.4	+4.4		
Jackson (1957)	0	+4.9	+4.2	+14.5	+8.0		
Mack	0	+4.7	+3	+ 6.7	+5		
Razumovskii and Chaika	0	+5.7	+4.2	+ 7.6	+4.7		
Jackson and Duong (1963*a*)	0	+7.7	+4.2	+ 8.4	+4.6	+7.4	+7.8
Jackson and Duong (1963*b*)	0	+7.0	—	+ 8.1	—		

Arroe also studied the structures of the resonance lines of the spark spectrum of Ba, λ 4934, 4554 ($6s\ ^2S_{1/2}$–$6p\ ^2P_{1/2,3/2}$), using the same method. In these lines the magnetic hyperfine structures of the odd isotopes are large and the centroids must be calculated. The resulting isotope shifts are tabulated in Table IV. The observed isotope shifts are larger than those observed in the

TABLE IV

Isotope shift in Ba II (mK) λ4934 ($6s\ ^2S_{1/2}$–$6p\ ^2P_{1/2}$), λ4554 ($6s\ ^2S_{1/2}$–$6p\ ^2P_{3/2}$)

	138	137	136	135	134
Arroe λ4934	0	+ 6.0	+4.8	+11.1	+ 9.6
Arroe λ4554	0	+ 6.4	+5.4	+12.6	+10.8
Crawford *et al.* λ4554	0	+13	+9	+19	—
Kelly and Tomchuk λ4934	0	+ 9.5	+7.8	+13.4	+ 8.5
Kelly and Tomchuk λ4554	0	+ 8.4	+7.8	+12.6	+ 8.5

arc line. From the point of view of interpretation of the results in terms of nuclear-volume effect (Kopfermann 1958) difficulties arise because neither the order of the isotopes found in Ba I and Ba II nor the ratios giving the relative shifts between the isotopes are the same.

As yet unpublished results on the structure of λ 5535 were obtained by Crawford *et al.* (1950) who employed an atomic beam in emission. This group found a strong component and satellites at +9.7 and +17.2 mK. The intensity ratios were found to be 72:14:6. These results are in rough agreement with those of Kopfermann and Wessel.

This group also studied the structure of the Ba II resonance line λ 4554. The resolution of the magnetic hyperfine structure was not complete and Arroe's (1950) value for the splittings of the $^2S_{1/2}$ level was used to calculate the centroids of the odd isotopes. A wing on the high-frequency side of the strong component was assigned to 136. The centroids of 137, 136, and 135 were found to be at 13±3, 9±1, and 19±3 mK relative to 138.

An investigation by Jackson (1957) used the absorption of the resonance line in three atomic beams each with a high collimation ratio of 28:1. Jackson observed components at 0.0, +3.8, +9.9, and +18.4 mK with intensities 20:4.5:2.5:1. In order to fit the observed spacings and intensities, Jackson assigned a magnetic hyperfine structure splitting to the $^1P_1$ levels of the two odd isotopes but used positive A factors for the magnetic structure.

Mack (1958), in an attempt to resolve the inconsistencies in the data for λ 5535, used negative A factors, as predicted by the theory of Breit and Wills (1933) (see Kopfermann 1958, p. 152) for the magnetic hyperfine structure of the $^1P_1$ levels of the odd isotopes. The wide structure observed by the atomic beam methods was explained by the magnetic hyperfine structure of the odd isotopes and the small isotope shifts found by Arroe were preserved, except for a rearrangement of the order of the isotopes. Mack's order of the isotopes is the same as that observed by Arroe in Ba II. Mack was unable to reconcile his pattern completely with observed intensities.

During the progress of our experiments, further atomic beam results were obtained (Jackson 1961) and two additional studies using enriched isotopes were made (Razumovskii and Chaika 1962; Jackson and Duong 1963*a*). The results of these experiments are given in Tables II and III. The order of the isotopes in all the experiments with enriched isotopes on the shifts in λ 5535 is the same, although there are differences in the observed magnitudes. This order in λ 5535 is different from the observation of Arroe using the same method on the Ba II resonance lines. The isotopic orders in the various experiments are collected in Table V.

TABLE V

Order of the isotopes

	138	137	136	135	134
Arroe (Ba I)	1	4	2	5	3
Arroe (Ba II)	1	3	2	5	4
Crawford *et al.* (Ba II)	1	3^{+1}_{-0}	2	4^{+1}_{-0}	–
Jackson (1957) (Ba I)	1	3	2	5	4
Mack (Ba I)	1	3	2	5	4
Razumovskii and Chaika (Ba I)	1	4	2	5	3
Jackson and Duong (1963*a*) (Ba I)	1	4	2	5	3
Kelly and Tomchuk (Ba II)	1	4	2	5	3

A further experiment of Jackson and Duong (1963*b*) employed an atomic beam of enriched odd isotopes to absorb λ 5535 within a spherical Fabry–Pérot interferometer. This experiment gives accurate values of the magnetic splitting factors, A, and the quadrupole–moment coupling factors, B, for both odd isotopes and places the positions of isotopes 137 and 135 at +7.0±0.3 and 8.1±0.3 mK relative to 138.

EXPERIMENTAL ARRANGEMENTS

The light source was an atomic beam excited by electron collision and viewed at right angles to the axis of the beam. For λ 5535 the collimation of the beam

was 25:1 and the calculated source line width was 0.001 cm^{-1}. For λ 3072, λ 4934, λ 4554 several collimations between 15:1 and 25:1 were used. These correspond to source line widths between 1 and 2 mK. A Fabry–Pérot interferometer was mounted in front of the slit of a Hilger medium quartz spectrograph which served to isolate the lines studied. For λ 5535, the interferometer plates were coated with silver with a reflection coefficient of 0.95, giving a resolving limit of about 1/60 of an order (Kuhn and Wilson 1950). Silver coatings were also used for λ 4554 and λ 4934, but aluminum films were used for the ultraviolet line λ 3072.

λ 5535 was recorded on Kodak 103aD plates, while 103aJ plates were used for λ 4934 and 103aO plates for λ 4554 and λ 3072.

RESULTS

The resonance line of Ba I (λ 5535) was studied with a 10-cm etalon. A strong component, A, and three satellites, B, C, D, were observed. The positions of the satellites relative to A were measured with a comparator and a microphotometer and were found to be 4.4±0.3, 10.0±0.3, and 18.6±0.3 mK.

The relative intensities of the components were determined from photometer tracings and were found to be 14:4.5:4:1 with an uncertainty of about 20%. The presence of the strong component A makes a large background correction for B and C which must be estimated from the shape of the interference fringes and could include a systematic error. Self-absorption in our source tends to make the intensities of the components more nearly equal, but should not affect the positions of the components.

The exposure times for λ 5535 varied from ½ to 1½ hours with a few exposures of 7 hours to search for the component near +24 mK suggested by Kopfermann and Wessel (1948). We were not able to find a component at this position in agreement with Jackson's (1957) result. The photometer contours of the fringes indicated the presence of the other component found by Jackson (1961) between our components A and B, but our resolution was not sufficient to give a numerical value to its position.

The structure of the second member of the principal singlet series in Ba I, λ 3072 ($6s^2\ {}^1S_0$–$6s7p\ {}^1P_1$), was studied with a 10-cm etalon. No clear resolution of structure was observed but a wing on the high-frequency side of the fringes 15 mK wide was found.

The structure of the resonance lines of Ba II λ 4934, 4554 ($6s\ {}^2S_{1/2}$–$6P\ {}^2p_{1/2,3/2}$) have also been studied with a variety of etalons. In λ 4934 both the ${}^2S_{1/2}$ and ${}^2P_{1/2}$ hyperfine structures could be resolved so that each odd isotope gives four components with intensity ratios 5:5:1:5. Energy-level diagrams are given in Fig. 1. Patterns were obtained using 2.5, 4.3, and 10.0 cm etalons. From these measurements the magnetic splittings for the ${}^2S_{1/2}$ level are 239.5±0.4 and 269.1±0.6 mK for 135 and 137. The ratio of these is 1.124±0.005, which agrees within experimental error with the more accurate result, 1.119, from magnetic resonance experiments (Hay 1941; Walchi and Rowland 1956). The splittings of the ${}^2P_{1/2}$ levels were found to be 46.9±1.5 and 51.1±0.6 mK for 135 and 137. The ratio is 1.09±0.05, which

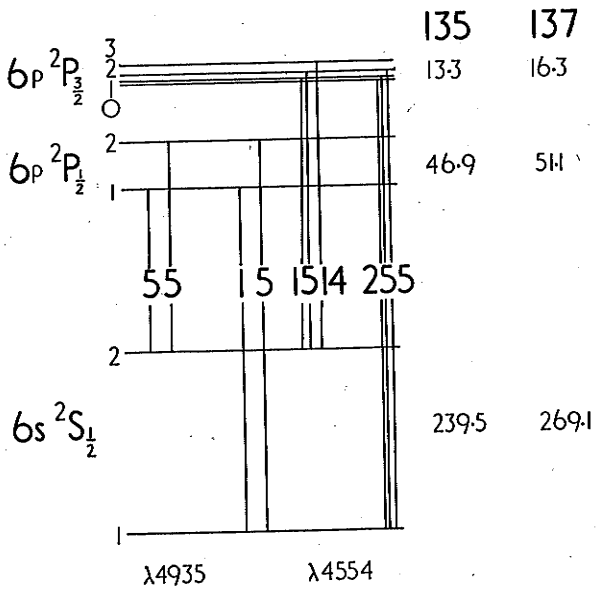

FIG. 1. Magnetic hyperfine structure in λ 4935 and λ 4554 of Ba II.

also agrees within experimental error with the ratio determined by the resonance methods.

Table VI compares our results for λ 4934 with those of Arroe (1950). Our values of the $^2S_{1/2}$ hyperfine structure are somewhat smaller than those of Arroe and the differences between the two results are a little larger than the

TABLE VI

Magnetic h.f.s. in λ4934 (mK)

	135	137	Ratio
$^2S_{1/2}$			
Arroe	243±1	271±1	1.115±0.005
Kelly and Tomchuk	239.5±0.4	269.1±0.6	1.124±0.005
$^2P_{1/2}$			
Arroe	41.5	46.3	1.113±0.005
Kelly and Tomchuk	46.9±1.5	51.1±0.6	1.09±0.05

combined errors. In each case the ratio of the splittings agrees within experimental error with the more accurate value obtained from magnetic resonance experiments. Our values for the $^2P_{1/2}$ hyperfine structure are about 10% larger than those of Arroe. They are obtained from the measurement of sharp components without reference to the strong 138 component. Arroe's line widths were about 36 mK. This line width is close to the $^2P_{1/2}$ structure and may have influenced the result. Arroe's estimated error for his ratio for the $^2P_{1/2}$ splittings seems too small.

In λ 4554 the structure is more complex owing to the magnetic hyperfine structure of the $^2P_{3/2}$ levels. Each odd isotope has six components in two groups separated by the $^2S_{1/2}$ structure. The expected structure and component intensities are given in Fig. 1.

This line was studied with 1.773, 3.010, 4.999, and 8.009 cm etalons. The pattern for the 1.7-cm etalon gives two components for the odd isotopes with a separation of 241.4±1.5 mK. This is an average value for the two isotopes and the result agrees with earlier measurements of Crawford *et al.* (1950).

With the 3- and 5-cm etalons, resolution of some of the $^2P_{3/2}$ structure was obtained and the separations of the $F = 3$ and $F = 2$ hyperfine states were found to be 13.3±1.0 and 16.3±0.8 mK for 135 and 137 respectively. Here the ratio between the two values is 1.23, which differs from the more accurate ratio by 10%. However, the combined error of our measurements is 12%. The components were identified by their intensities and the value of the $^2S_{1/2}$ splitting measured in λ 4934. No independent value of the $^2S_{1/2}$ splitting was obtained from this line because of the uncertainties introduced by the $^2P_{3/2}$ structure.

The centroids of the odd isotopes relative to 138 can be determined from the observed data. They are found to be +9.5±1.0 and +13.4±1.3 for 135 and 137 in λ 4934, and +8.4±1.1 and +12.6±1.3 in λ 4554. These data are included in Table IV. The errors are estimates from average deviation from the means. The data for λ 4934 are considered to be the more reliable.

In the patterns with the largest etalons a weak wing at 8±1 mK was observed in both lines. This component appeared to be slightly broadened.

DISCUSSION

The results of Jackson and Duong (1963*b*) show conclusively that the structure observed in λ 5535 by atomic-beam methods is a combination of isotope shift and magnetic hyperfine structure. There is a very satisfactory fit between these results (1963*b*) and Jackson and Duong's (1963*a*) earlier isotope-shift determinations. Excepting Arroe's (1950) position of 136, there is also fair agreement among all the hollow-cathode enriched-isotope measurements. The patterns observed in atomic-beam measurements (Table II) can be predicted accurately from Jackson and Duong's (1963*b*) results.

The structure in λ 3072 observed in these experiments gives a qualitative confirmation. Since λ 3072 involves the same lower level ($6s^2\,{}^1S_0$) as λ 5535 and the upper level changes only by the excitation of the p electron from $6p$ to $7p$, the volume or field-effect shift can be expected to be the same or slightly decreased owing to the decreased screening of the $6s$ electron by the p electron. The isotope shift will be decreased by about 1 mK relative to λ 5535 because of changes in the normal mass shift. The formula of Breit and Wills (1933) gives a value of $A(6s6p\,{}^1P_1) = -3$ mK in agreement with the measured value of −3.6 mK (Jackson and Duong 1963*b*). For $6s7p\,{}^1P_1$ a similar calculation gives $A = -5$ mK with an uncertainty of at least 50%. The structure of λ 3072 can then be expected to be due almost entirely to

the magnetic hyperfine structure of the two odd isotopes. The weak high-frequency wing observed on a strong component fits the above estimates.

A major difficulty in the interpretation of the barium isotope-shift data is the lack of agreement in the order of the isotopes between Arroe's Ba II data and the observations made on λ 5535. In λ 5535 both the odd isotopes are shifted beyond 134, while in Ba II 137 lies between 136 and 134.

Our Ba II data are not entirely conclusive on the relative positions of the isotopes. The intensity of the wing on the high-frequency side of the component due to 138 indicates that the wing is due to the unresolved components of 136 and 134. The components can be given weight factors equal to their relative abundances (Table I). Since the shifts are caused almost entirely by volume and field effects of the nucleus, the ratio of the shifts of the two isotopes relative to 138 should be the same as that observed in λ 5535 of Ba I, that is 4.2:4.6 (Table III). Then the calculated positions of 136 and 134 are +7.8 and +8.5 relative to 138. The uncertainty in these values is estimated to be 1.2 mK.

In λ 4934 the most probable position of 137 is beyond 134, although the combined errors of the positions are larger than the difference. In λ 4554 the positions of 137 and 134 are reversed, but the combined errors (2.3 mK) are many times the difference (0.1 mK). Because of the difficulty in determining accurately the $^2P_{3/2}$ magnetic hyperfine structure and the incomplete resolution of all the components in the pattern, we estimate that the λ 4554 data are more likely to contain systematic error. The most probable order of isotopes in our Ba II data is that of λ 4934, which is the same as the order assigned in the hollow-cathode enriched-isotope experiments.

There are a number of reasons for a difference in the magnitude of the shifts between Ba I and Ba II. The normal mass shifts are proportional to frequency and thus are larger in the Ba II lines. This difference can, however, be readily calculated and for the isotope pair 137–135 the Ba II results should be reduced by 0.2 mK before comparison with Ba I. The specific mass effect may give a small contribution, but neither the magnitude nor the sense can be estimated with sufficient accuracy from present methods. The expectation, however, is that the effect is small (Kelly and Tomchuk 1961). Self-absorption of λ 5535 in the hollow cathode is a possible cause of a reversal in the order of isotope pairs, but Jackson and Duong (1963*a*) estimate the effect to be small. This is borne out by the good agreement between the results of Jackson and Duong (1963*a*, *b*) using two different methods.

In mercury the shift of a $6s^2$ configuration is 1.6 times that of the $6s$ configuration (Kopfermann 1958, p. 173) owing to the mutual screening of the two $6s$ electrons. The shifts in the Ba II resonance lines can then be expected to be about 40% larger than in the Ba I resonance line.

Our average shift in Ba II between 137 and 135 is 4.0±2.3 mK. Arroe's corresponding value is 5.6±1.4. In Ba I Jackson and Duong (1963*b*) observe a shift of 1.1±0.6 mK. If our Ba II result is decreased by 40%, it becomes 2.6±2.3. The difference between this and the Ba I measurement is one half the combined errors. Our best value of the shift between 138 and 137 in Ba II

is 9.5±1.0 mK. Jackson and Duong (1963*b*) find this shift in Ba I to be 7.0 ±0.3 mK. If the Ba II result is decreased by 40%, it becomes 5.7±1.0 mK. The difference between this value and the Ba I data is within the combined errors of the measurements. Arroe's value of the 138–137 shift is 6.4±0.7 mK. If this is decreased by 40%, the difference between Arroe's Ba II value and the Ba I data is three times the combined error. As pointed our by Razumovskii and Chaika (1962), Arroe's result may be influenced by an attempt to keep the spacings of the even isotopes uniform.

CONCLUSIONS

The unusual order of the isotopes of barium observed in the Ba I resonance line, where the isotope shift due to removal of a single neutron from Ba^{138} to make Ba^{137} is greater than the shift due to the removal of four neutrons to form Ba^{134}, is confirmed in part by observation on the Ba II resonance lines. The magnitude of the isotope shift for a change of two neutrons is strongly dependent on the neutron number.

ACKNOWLEDGMENTS

This research was supported by a grant from the National Research Council of Canada. The authors are grateful to Dr. A. E. Douglas of the National Research Laboratory, Ottawa, for making microphotometer traces of the interference patterns.

REFERENCES

ARROE, A. H. 1950. Phys. Rev. **79**, 836.
BREIT, G. and WILLS, L. A. 1933. Phys. Rev. **44**, 740.
CRAWFORD, M. F., KELLY, F. M., and KURZ, W. 1950. Unpublished data, University of Toronto.
HAY, R. H. 1941. Phys. Rev. **60**, 75.
JACKSON, D. A. 1957. Phys. Rev. **106**, 948.
——— 1961. Proc. Roy. Soc. (London), Ser. A, **263**, 289.
JACKSON, D. A. and DUONG, H. T. 1963*a*. Proc. Roy. Soc. (London), Ser. A, **274**, 145.
——— 1963*b*. Phys. Rev. Letters, **11**, 209.
KELLY, F. M. and TOMCHUK, E. 1961. Proc. Phys. Soc. (London), **78**, 1304.
KOPFERMANN, H. 1958. Nuclear moments (Academic Press, New York).
KOPFERMANN, H. and WESSEL, G. 1948. Nachr. Akad. Wiss. Göttingen, Math-Physik, Kl. IIa, No. 2, 53.
——— 1951. Nachr. Akad. Wiss. Göttingen, Math-Physik, Kl. IIa, No. 3, 1.
KUHN, H. and WILSON, B. A. 1950. Proc. Phys. Soc. (London), **B63**, 745.
MACK, J. E. 1958. Phys. Rev. **109**, 820.
RAZUMOVSKII, A. N. and CHAIKA, M. P. 1962. Opt. i Spektroskopiya, **12**, 338 (Opt. Spectr. USSR, English Transl. **12**, 186).
WALCHI, H. E. and ROWLAND, T. J. 1956. Phys. Rev. **102**, 1334.